Chemistry of Iron with Dipicolinic Acid. 2. Bridging Role of Carboxylate Groups in Solid State Structures

P. Lainé, A. Gourdon,* and J.-P. Launay

Molecular Electronics Group, CEMES, CNRS UP8011, BP4347, 29 Rue J. Marvig, 31055 Toulouse Cedex, France

Received January 27, 1995[⊗]

This paper reports the syntheses, structures, and properties of iron(II) and dipicolinic acid oligonuclear complexes prepared in slightly acidic medium. Acidification of $[(dipic)_2Fe^{II}]Na_2 \cdot 2H_2O$ or reaction of $dipicH_2$ (2,6-pyridine dicarboxylic acid) and Mohr's salt (ammonium iron(II) sulfate hexahydrate) at pH 5.3 yielded $[(dipic)_2(dipicH)_2Fe^{II}_3(OH_2)_4] \cdot 2H_2O$ (**1**), which consists of two $[(dipic)(dipicH)Fe^{II}]$ fragments sharing one oxygen atom each with a $[Fe^{II}(OH_2)_4O_2]$ subunit. Reaction of $dipicH_2$ and Mohr's salt at pH 6.25 gave the dinuclear species $[(dipic)_2Fe^{II}_2(OH_2)_5]$ (**2**), in which a $[(dipic)_2Fe^{II}]$ moiety shares one oxygen atom with a $[Fe^{II}(OH_2)_5O]$ fragment. When the reaction was conducted at pH 5.85, the reaction gave crystals of $[(dipic)_4(dipicH_2)_2Fe^{II}_3(OH_2)_6](NH_4)_2 \cdot 4H_2O$ (**3**), which contains, in the unit cell, both the reactants $[Fe^{II}(OH_2)_6]^{2+}$ and $dipicH_2$ and the product $[(dipic)_2Fe^{II}]^{2-}$. At pH 5.65, the reaction yielded crystals of $[(dipic)_{10}(dipicH)_6Fe^{II}_{13}(OH_2)_{24}] \cdot 13H_2O$ (**4**), which contains, in the same unit cell, one trinuclear anionic complex $\{[(dipic)_2Fe^{II}]-[Fe^{II}(OH_2)_4]-[Fe^{II}(dipic)_2]\}^{2-}$, two doubly protonated cationic dinuclear complexes $\{[(dipicH)Fe^{II}(dipicH)]-[Fe^{II}(OH_2)_5]\}^{2+}$, two singly protonated cationic dinuclear complexes $[(dipicH)Fe^{II}(dipic)]-[Fe^{II}(OH_2)_5]^{+}$, and two mononuclear anionic complexes $[(dipic)_2Fe^{II}]^{2-}$. The crystal structures for **1**−**4** have been solved: **1** crystallized in the monoclinic space group $P2_1/n$ with $a = 8.956(3)$ Å, $b = 15.083(7)$ Å, $c = 12.504(5)$ Å, $\beta = 90.42(8)°$, $V = 1689(1)$ Å^3, and $Z = 2$. **2** was found in the triclinic space group $P\bar{1}$ with $a = 8.339(2)$ Å, $b = 9.711(2)$ Å, $c = 13.994(4)$ Å, $\alpha = 100.75(4)°$, $\beta = 101.99(2)°$, $\gamma = 97.04(2)°$, $V = 1076(13)$ Å^3, and $Z = 2$. **3** crystallized in the triclinic space group $P\bar{1}$ with $a = 10.759(2)$ Å, $b = 10.917(3)$ Å, $c = 12.653(3)$ Å, $\alpha = 105.62(2)°$, $\beta = 96.25(2)°$, $\gamma = 103.25(2)°$, $V = 1370(11)$ Å^3, and $Z = 1.4$ was found in the triclinic space group $P\bar{1}$ with $a = 15.700(4)$ Å, $b = 15.811(4)$ Å, $c = 16.558(5)$ Å, $\alpha = 85.49(2)°$, $\beta = 67.75(2)°$, $\gamma = 76.47(3)°$, $V = 3698(15)$ Å^3, and $Z = 1$.

Introduction

In the previous paper, we obtained some evidence that the free oxygen of the carboxylate groups of $[(dipic)_2Fe^{II}]^{2-}$ had some Lewis base character. This led us to study the acidification of the above complex or, more generally, the chemistry of iron(II) and dipicolinic acid in slightly acidic medium. Surprisingly, we found that minute changes in the preparation procedures gave a series of complicated structures, with a common point: the bridging role of carboxylate groups and/or hydrogen bonds. Four of these structures, in which iron is hexacoordinated, are described below (heptacoordinated species are described in paper 3 of this series).

Experimental Section

Most of the experimental techniques and conditions have been described in the previous paper of this issue.[1] All pH measurements were performed at room temperature with a calibrated Hanna 8520 pH-meter.

Synthesis of $[(dipic)_2(dipicH)_2Fe^{II}_3(OH_2)_4]$. Route A: Synthesis from $[(dipic)_2Fe^{II}]Na_2$. $[(dipic)_2Fe^{II}]Na_2 \cdot 2H_2O$ (1 g, 2.14 mmol) was dissolved in 90 mL of degassed water (initial pH 6.92). The solution was then concentrated to 25 mL by heating under argon and acidified to pH 3.5 by dropwise addition of a 0.1 M degassed aqueous solution of HCl. After 10 min of stirring, the heating was stopped and the solution was left to cool slowly, yielding 250 mg of $[(dipic)_2(dipicH)_2Fe^{II}_3(OH_2)_4]$ (37%). Anal. Calcd for $C_{28}H_{26}N_4Fe_3O_{22}$: C, 36.85; H, 2.79; N, 5.97; Fe, 17.86. Found: C, 36.79; H, 2.78; N, 5.95; Fe, 17.82. FTIR (KBr, cm^{-1}): 3427 br, vs (ν OH); 1654 (ν_{asym} COO from COOH); 1624, 1590, 1573 (ν_{asym} COO from COO$^-$); 1466, 1431 (ν_{sym} COO$^-$). UV−vis in H_2O, pH 6.75 (λ_{max}, nm ($10^{-2}\epsilon$, dm^3 mol^{-1} cm^{-1})): 456 (21); 267 (200).

Route B: Direct Synthesis. An aqueous (50 mL) suspension of $dipicH_2$ (6.51 g, 38.89 mmol) at 100 °C was neutralized under argon with concentrated sodium hydroxide aqueous solution (final pH 6.7). To this pasty mixture, heated to liquefaction by an oil bath at 120 °C, was added dropwise an aqueous solution of hydrochloric acid to pH 5.30. At this stage, the mixture was nearly solid; then 11.51 g of Mohr's salt (29.37 mmol) was added. The deep orange-red mixture liquefied instantly, was stirred 10 min with heating, and then was left to cool for 24 h. The dark-red needles so obtained were then washed with diethyl ether and dried under vacuum. Yield: 7.5 g, 82%. Further cooling of the mother liquors yielded a crop of impure product containing white crystals of $dipicH_2$.

Synthesis of $[(dipic)_2Fe^{II}_2(OH_2)_5]$. An aqueous supension (65 mL) of $dipicH_2$ (4.2 g, 24.13 mmol) was treated with aqueous NaOH up to pH 6.25 (final volume 90 mL). To the heated solution (100 °C) was then added Mohr's salt (8.5 g, 21.67 mmol). The deep red mixture was heated with stirring for 0.5 h and left to cool to room temperature, giving 3.65 g (6.37 mmol, 59%) of large deep red crystals. Anal. Calcd for $[(dipic)_2Fe^{II}_2(OH_2)_5] \cdot 2.25H_2O$ ($C_{14}H_{20.5}N_2Fe_2O_{15.25}$): C, 29.37; H, 3.61; N, 4.89; Fe, 19.51. Found: C, 29.25; H, 3.55; N, 4.91; Fe, 19.70. FTIR (KBr pellets, cm^{-1}): 3233 (ν OH); 1614, 1588, 1571 (ν_{asym} COO from COO$^-$); 1431, 1394 (ν_{sym} COO$^-$).

Synthesis of $[(dipic)_4Fe^{II}_3(OH_2)_6](NH_4)_2(dipicH_2)_2$. A suspension of $dipicH_2$ (5 g, 29.92 mmol) in degassed water (50 mL) at 95 °C was treated with a concentrated aqueous solution of NaOH up to pH 5.85 (final volume around 65 mL). Addition of Mohr's salt (10.3 g, 26.27 mmol) gave a deep red solution, which was stirred with heating for 1/4 h and left to cool to room temperature. Crystallization started immediately. After 12 h, the crystals of $[(dipic)_4(dipicH_2)_2Fe^{II}_3(OH_2)_6](NH_4)_2$ were filtered off under argon, washed with acetone and then diethyl ether, and dried (5.95 g, 49%). Several grams of less pure product could be obtained by further cooling (4 °C) of the mother liquor. Anal. Calcd for $[(dipic)_4(dipicH_2)_2Fe^{II}_3(OH_2)_6](NH_4)_2 \cdot 4H_2O$ ($C_{42}H_{50}N_8Fe_3O_{34}$): C, 36.59; H, 3.65; N, 8.13; Fe, 12.15. Found: C,

[⊗] Abstract published in *Advance ACS Abstracts*, September 15, 1995.

(1) *Inorg. Chem.* **1995**, *34*, 5129.

0020-1669/95/1334-5138$09.00/0

Table 1. Crystallographic Data for $[(dipic)_2(dipicH)_2Fe^{II}_3(OH_2)_4]\cdot 2H_2O$ (**1**), $[(dipic)_2Fe^{II}_2(OH_2)_5]\cdot 2.25H_2O$ (**2**), $[(dipic)_4Fe^{II}_3(OH_2)_6](NH_4)_2]\cdot 4H_2O\cdot 2dipicH_2$ (**3**), and $[(dipic)_{10}(dipicH)_6Fe^{II}_{13}(OH_2)_{24}]\cdot 13H_2O$ (**4**)

	1	**2**	**3**	**4**
	$C_{28}H_{26}N_4Fe_3O_{22}$	$C_{14}H_{20.5}N_2Fe_2O_{15.25}$	$C_{42}H_{50}N_8Fe_3O^{34}$	$C_{112}H_{122}N_{16}Fe_{13}O_{101}$
fw	938.07	572.51	1378.43	4052.27
space group	$P2_1/n$ (No. 14)	$P\bar{1}$ (No. 2)	$P\bar{1}$ (No. 2)	$P\bar{1}$ (No. 2)
a, Å	8.956(3)	8.339(2)	10.759(2)	15.700(4)
b, Å	15.083(7)	9.711(2)	10.917(3)	15.811(4)
c, Å	12.504(5)	13.994(4)	12.653(3)	16.558(5)
α, deg	90	100.75(4)	105.62(2)	85.49(2)
β, deg	90.42(8)	101.99(2)	96.25(2)	67.75(2)
γ, deg	90	97.04(2)	103.25(2)	76.47(3)
V, Å^3	1689(1)	1076(13)	1370(11)	3698(15)
Z	2	2	1	1
T, °C	21	21	21	21
μ(Mo Kα), cm^{-1}	13.69	14.24	8.89	13.55
ϱ_{cal}, g cm^{-3}	1.84	1.765	1.67	1.81
R^a	0.022	0.0260	0.0313	0.0559
$R_w{}^b$	0.024	0.0272	0.0332	0.0657

^{a} $R = \sum||F_o| - |F_c||/\sum|F_o|$. ^{b} $R_w = [\sum w(|F_o| - |F_c|)^2/\sum w|F_o|2]^{1/2}$.

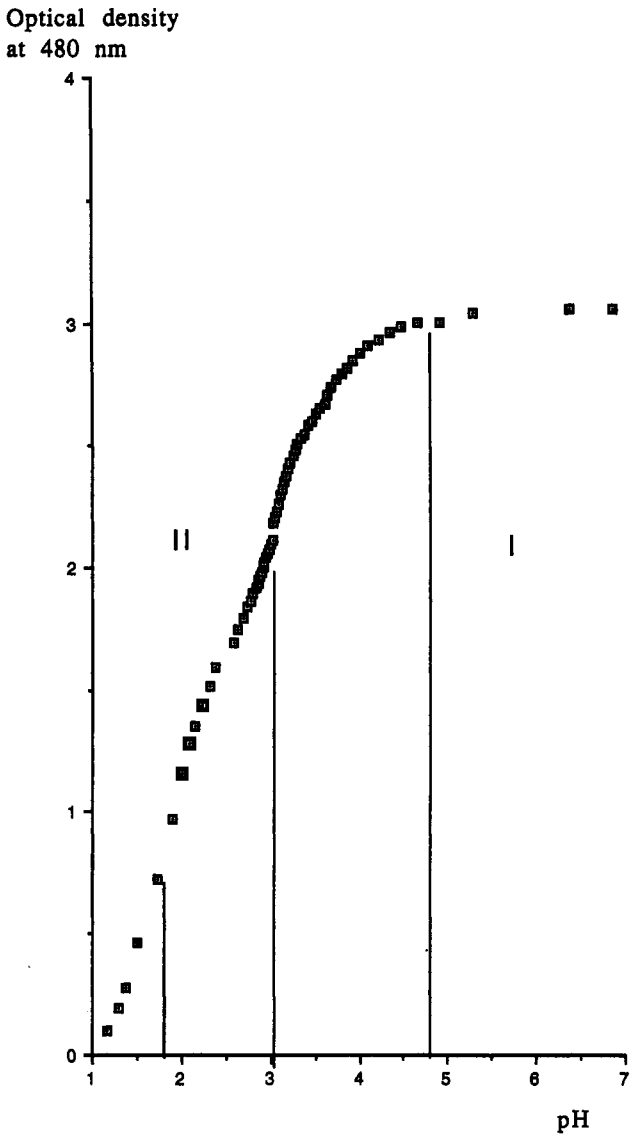

Figure 1. Variation of the optical density at 480 nm of a 9 × 10^{-3} M aqueous solution of $[(dipic)_2Fe^{II}]Na_2\cdot 2H_2O$ as function of pH.

36.41; H, 3.57; N, 8.06; Fe, 11.97. FTIR (KBr pellets, cm^{-1}): 3503, 3204 br, vs (ν OH); 1715 (ν_{asym} COO from COOH); 1621, 1588, 1570 (ν_{asym} COO from COO$^-$); 1435, 1397, 1388 (ν_{sym} COO).

Synthesis of $[(dipic)_{10}(dipicH)_6Fe^{II}_{13}(OH_2)_{24}]\cdot 13H_2O$. A suspension of dipicH$_2$ (9.75 g, 58.34 mmol) in degassed water (75 mL) at 100 °C was treated with concentrated aqueous NaOH up to pH 5.65 (final volume *ca* 100 mL). To the refluxing solution was then added 17.25 g of Mohr's salt (43.99 mmol). After being stirred for 10 min at this temperature, the dark red-orange mixture was left to cool to room temperature. After 12 h at room temperature, filtration gave 9.60 g of dark red-violet crystals of $[(dipic)_{10}(dipicH)_6Fe^{II}_{13}(OH_2)_{24}]\cdot 13H_2O$ (yield 70%). Cooling of the mother liquor to 4 °C provided 1.6 g of another compound which will be described in a following paper. Anal. Calcd for $C_{122}H_{122}N_6Fe_{13}O_{101}$: C, 33.45; H, 3.05; N, 5.55; Fe, 17.99. Found: C, 33.18; H, 3.07; N, 5.61; Fe, 17.73. FTIR (KBr pellets, cm^{-1}): 3254 br, vs (ν OH); 1618, 1590, 1573 (ν_{asym} COO from COO$^-$); 1430, 1376 (ν_{sym} COO$^-$).

Table 2. Selected Atomic Coordinates and Equivalent Isotropic Thermal Parameters (Å^2) for $[(dipic)_2(dipicH)_2Fe^{II}_3(OH_2)_4]\cdot 2H_2O$ (**1**)

atom	x/a	y/b	z/c	U(iso)^a
Fe(1)	0.0000	0.0000	0.5000	0.0240
O(110)	−0.1005(2)	−0.0225(1)	0.3447(2)	0.0369
O(120)	−0.2124(2)	−0.0025(2)	0.5672(2)	0.0387
Fe(2)	0.16421(4)	0.27852(3)	0.23505(3)	0.0289
N(1)	0.1872(2)	0.2270(1)	0.0798(1)	0.0245
C(1)	0.0163(3)	0.3430(2)	0.0391(2)	0.0273
C(2)	0.1126(3)	0.2673(2)	0.0014(2)	0.0253
C(3)	0.1242(3)	0.2404(2)	−0.1040(2)	0.0321
C(4)	0.2149(3)	0.1688(2)	−0.1266(2)	0.0370
C(5)	0.2930(3)	0.1270(2)	−0.0454(2)	0.0349
C(6)	0.2766(3)	0.1584(2)	0.0576(2)	0.0268
C(7)	0.3577(3)	0.1255(2)	0.1542(2)	0.0298
O(11)	0.0068(2)	0.3524(1)	0.1400(1)	0.0319
O(12)	−0.0459(2)	0.3901(1)	−0.0282(1)	0.0357
O(71)	0.3470(2)	0.1646(1)	0.2392(1)	0.0359
O(72)	0.4398(2)	0.0556(1)	0.1380(2)	0.0366
N(11)	0.1942(2)	0.3097(1)	0.3957(2)	0.0264
C(11)	0.3470(3)	0.4241(2)	0.3287(2)	0.0328
C(12)	0.2888(3)	0.3737(2)	0.4247(2)	0.0284
C(13)	0.3294(3)	0.3864(2)	0.5308(2)	0.0362
C(14)	0.2690(3)	0.3301(2)	0.6062(2)	0.0387
C(15)	0.1703(3)	0.2637(2)	0.5758(2)	0.0342
C(16)	0.1348(3)	0.2557(2)	0.4682(2)	0.0280
C(17)	0.0337(3)	0.1870(2)	0.4185(2)	0.0307
O(111)	0.3027(2)	0.3932(1)	0.2391(1)	0.0353
O(112)	0.4308(2)	0.4876(1)	0.3418(2)	0.0431
O(171)	0.0230(2)	0.1886(1)	0.3180(1)	0.0369
O(172)	−0.0328(2)	0.1355(1)	0.4801(2)	0.0385

^{a} Equivalent isotropic U(iso) defined as one-third of the trace of hte orthogonalized tensor.

X-ray Crystallography. Most X-ray crystallography experimental details can be found in ref 1. Experimental data are summarized in Table 1.

For $[(dipic)_2(dipicH)_2Fe^{II}_3(OH_2)_4]\cdot 2H_2O$ (**1**), the positioning of the two acidic protons was done in the following way: Bond lengths, Mössbauer spectroscopy, and magnetic studies (vide infra) indicated

Table 3. Selected Distances (Å) and Angles (deg) or $[(dipic)_2(dipicH)_2Fe^{II}_3(OH_2)_4]\cdot 2H_2O$ (**1**)

Fe(1)−O(110)	2.161(2)	C(1)−O(11)	1.273(3)
Fe(1)−O(120)	2.085(2)	C(1)−O(12)	1.232(3)
Fe(1)−O(172)	2.079(2)	C(7)−O(71)	1.221(3)
Fe(2)−N(1)	2.102(2)	C(7)−O(72)	1.302(3)
Fe(2)−O(11)	2.148(2)	C(11)−O(111)	1.275(3)
Fe(2)−O(71)	2.373(2)	C(11)−O(112)	1.227(3)
Fe(2)−N(11)	2.078(2)	C(17)−O(171)	1.260(3)
Fe(2)−O(111)	2.129(2)	C(17)−O(172)	1.248(3)
Fe(2)−O(171)	2.129(2)		
O(120)−Fe(1)−O(110)	89.09(8)	O(172)−Fe(1)−O(110)	90.61(8)
O(120)−Fe(1)−O(110)	90.91(8)	O9172)Fe(1)−O(120)	86.44(9)
O(120)−Fe(1)−O(110)	89.09(8)	O(172)− Fe(1)−O(120)	93.56(9)
O(172)−Fe(1)−O(110)	89.39(8)		
O(11)−Fe(2)−N(1)	75.49(7)	O(111)−Fe(2)−O(71)	100.73(7)
O(71)−Fe(2)−N(1)	71.36(7)	O(111)−Fe(2)−N(11)	73.88(7)
O(71)−Fe(2)−O(11)	146.84(6)	O(171)−Fe(2)−N(1)	106.08(7)
N(11)−Fe(2)−N(1)	164.37(8)	O(171)−Fe(2)−O(11)	102.12(7)
N(11)−Fe(2)−O(11)	119.79(7)	O(171)−Fe(2)−O(71)	86.57(7)
N(11)−Fe(2)−O(71)	93.35(7)	O(171)−Fe(2)−N(11)	75.31(7)
O(111)−Fe(2)−N(1)	105.12(7)	O(171)−Fe(2)−O(111)	148.67(7)
O(111)−Fe(2)−O(11)	88.37(7)		

that all three iron atoms were at the oxidation state II. Electroneutrality of the crystals then required the neutralization of 2 charges in excess in the formula $[(dipic)_4Fe^{II}_3(OH_2)_4]^{2-}$, which, in the absence of heavy cations in difference Fourier syntheses and chemical analyses, were attributed to protons. These protons could then be located either on the crystallization water molecules or on two dipic ligands. The distortions of the iron environment (see Results and Discussion) allowed us to conclude that the two protons were linked to the ligands. They were located as the highest peaks on the difference Fourier maps.

For $[(dipic)_2Fe^{II}_2(OH_2)_5]$ (**2**), the number of crystallization water molecules was determined by refining the three of the oxygen atom occupation factors with fixed temperature factors (0.05 Å^2). Two of these factors refined to unity and the last one (O(300)) refined to 0.25, values to which they were fixed in the next steps of the refinements. These values are in good agreement with chemical analysis. All the H atoms, except those linked to the dipic ligands and to O(300), were localized by Fourier difference maps, and their positions were refined.

For $[(dipic)_4Fe^{II}_3(OH_2)_6](NH_4)_2\cdot 4H_2O\cdot 2dipicH_2$ (**3**), the asymmetric unit contains half a complex around one origin. All the H atoms, except those linked to pyridine rings of the dipic ligands, were localized by Fourier difference maps, and their positions were refined.

For $[(dipic)_{10}(dipicH)_6Fe^{II}_{13}(OH_2)_{24}]\cdot 13H_2O$ (**4**), the oxygen O(200) occupation factor was determined as above and converged to 0.5, the value to which it was fixed. Due to the large number of atoms and to the poor quality of the crystal, some water hydrogen atoms and the acidic H atoms were not localized.

For all four compounds, the data were not corrected for absorption effects. Selected atomic coordinates are in the Tables 2, 4, 7, and 10. Selected bond lengths and angles are gathered in the Tables 3, 5, 8, and 11.

Results and Discussion

Syntheses of $[(dipic)_2(dipicH)_2Fe^{II}_3(OH_2)_4]$. The solvatochromic properties of $[(dipic)_2Fe^{II}](TPA)_2$ (see ref 1) showed that the complex is a Lewis base and led us to study the acidification of this compound, and more generally the syntheses of products obtained from Fe^{2+} and $dipicH_2$ in *acidic medium*.

During the acidification of $[(dipic)_2Fe^{II}]^{2-}$ in aqueous solution, the analysis of the optical density (in the region of the metal-to-ligand charge transfer band) as a function of pH shows two regimes (Figure 1). Above pH 4.75, the spectra do not change and the complex seems stable. Below this value, the optical density decreases, showing that the complex is either decomposed or transformed into a less absorbing species. Considering that the optical density is proportional to the remaining concentration of the $[(dipic)_2Fe^{II}]^{2-}$ chromophore, the overall decomposition seems to occur in two steps. We have not been able however to write simple equations for this decomposition. In particular, there is no obvious relation between the solution behavior and the structures obtained in the solid state and described below.

For preparative purposes, the acidification of $[(dipic)_2Fe^{II}]Na_2$ was performed down to pH 3.5 after concentration. Slow crystallization gave the trinuclear complex $[(dipic)_2(dipicH)_2Fe^{II}_3(OH_2)_4]$, whose structure is described below. This species can also be prepared in good yield (82%) by direct reaction of $dipicH_2$ with Mohr's salt at carefully controlled pH, i.e 5.3, before addition of Mohr's salt. A number of such direct preparations have been performed, and we have found that

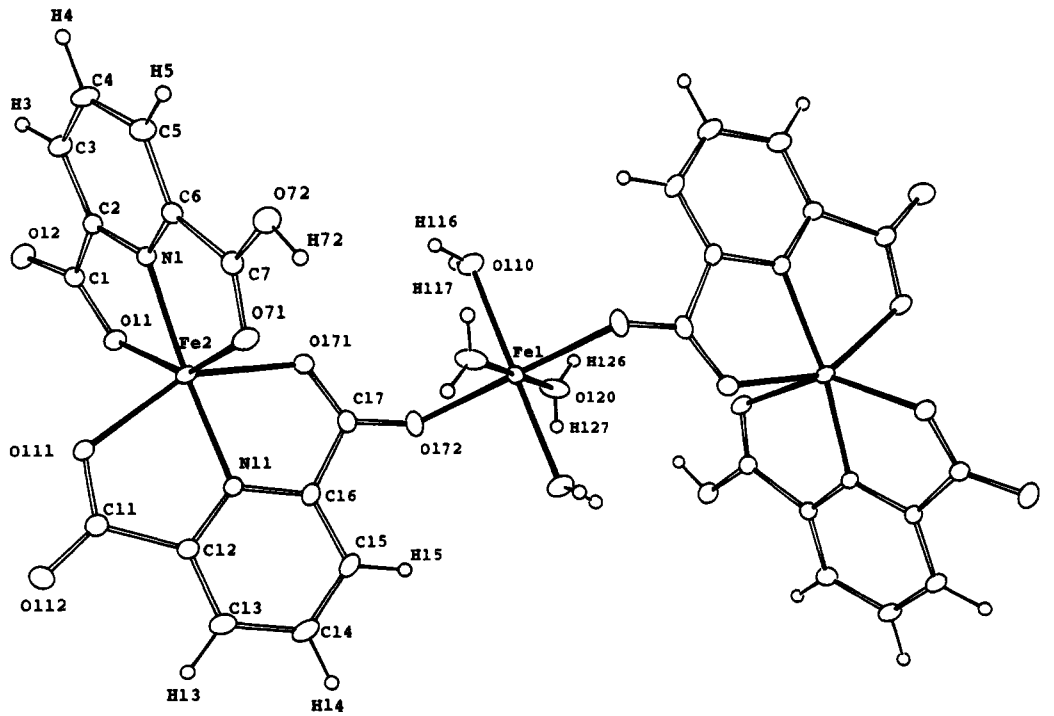

Figure 2. ORTEP plot of **1**. The molecule is symmetrical with respect to a crystallographic inversion center on Fe(1).

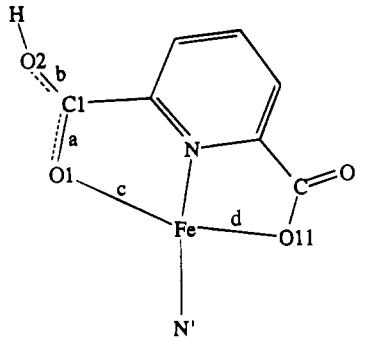

Figure 3. Consequences of the protonation of a dipic ligand on the geometry in the complex.

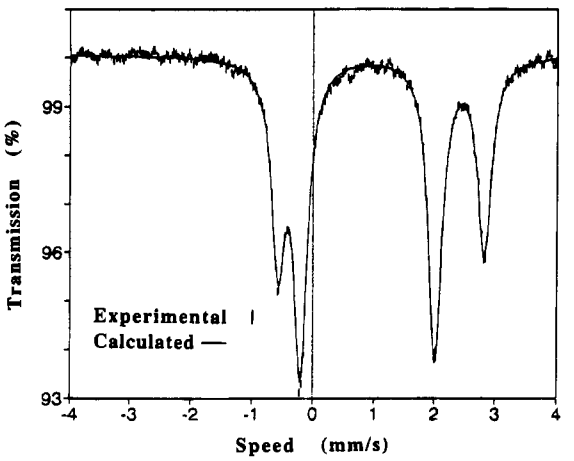

Figure 4. Mössbauer spectrum of **1** at 293 K. The solid curve through the experimental data has been calculated with the best fitting parameters reported in the text.

curiously the pH is the master parameter, while the Fe^{II}/dipicH$_2$ ratio has almost no effect in the range $0.5 < n_{Fe}/n_{dipic} < 1.0$.

This trinuclear complex is not stable in water (dilute solution) and decomposes on redissolution according to

$$[(dipic)_2(dipicH)_2Fe^{II}{}_3(OH_2)_4] + 5H_2O \rightarrow 3[(dipic)Fe^{II}(OH_2)_3] + dipicH_2 \quad (1)$$

Stucture of [(dipic)$_2$(dipicH)$_2$Fe$^{II}{}_3$(OH$_2$)$_4$] (1). [(dipic)$_2$-(dipicH)$_2$Fe$^{II}{}_3$(OH$_2$)$_4$] crystallizes in the centrosymmetric space group $P2_1/n$. Selected bond lengths and angles are grouped in Table 3. The asymmetric unit contains half a molecule located on a crystallographic inversion center on Fe(1) as shown on Figure 2 and a crystallization water molecule in general position. The structure consists of two [(dipic)(dipicH)Fe^{II}] subunits sharing one oxygen atom each with a [O$_2$Fe^{II}(OH$_2$)$_4$] fragment.

The coordination sphere around Fe(1) is distorted with an elongation in the Fe(1)−O(110) direction as shown by the distances Fe(1)−O(110) = 2.161(1) Å, Fe(1)−O(120) = 2.085(2) Å, and Fe(1)−O(172) = 2.079(2) Å. As observed for [(dipic)Fe^{II}(OH$_2$)$_3$], the shortest bond corresponds to a geometry in which the metal, the oxygen, and the two H atoms are coplanar (sums of the angles around the oxygen: 359° for O(120) and 335° for O(110)). Furthermore O(110) is not involved in hydrogen bonding, whereas O(120) is linked to the oxygen atom O(111) of an another molecule with O(11)−O(120) = 2.71(3) Å and O(11)−H(127) = 1.98(4) Å. The geometry of the two [(dipic)(dipicH)Fe^{II}] subunits is very close to that of [(dipic)$_2$Fe^{II}]$^{2-}$. The acidic H atom is linked by hydrogen bonding to the water molecule with distances H(72)−O(100) = 1.64(4) Å and O(72)−O(100) = 2.556(3) Å. The protonation of one of the carboxylate groups modifies (see Figure 3) the bonding in the complex by the following: (i) a shortening of **a**, here C(7)−O(71) (1.221(3) Å to compare with 1.260(3), 1.279(3), and 1.275(3) Å for the similar C−O bonds); (ii) a loss of **b** (here C(7)−O(72)) double bond character (1.302(3) Å to compare with C(1)−O(12) = 1.232(3) Å, C(11)−O(112) = 1.227(3) Å, and C(17)−O(172) = 1.248(3) Å); (iii) a lengthening of the **c** bond, Fe(2)−O(71), 2.373(2) Å whereas the other Fe−O bond (**d**) ranges from 2.129(3) to 2.148(2) Å. It allows a relaxation of the compression of the Fe−N bond

Table 4. Selected Atomic Coordinates and Equivalent Isotropic Thermal Parameters (Å^2) for [(dipic)$_2$Fe$^{II}{}_2$(OH$_2$)$_5$]·2.25H$_2$O (**2**)

atom	*x/a*	*y/b*	*z/c*	*U*(iso)[a]
Fe(1)	−0.17741(4)	0.11546(3)	0.20206(2)	0.0237
O(110)	−0.4036(2)	0.2120(2)	0.1805(1)	0.0304
O(120)	−0.3079(2)	−0.0365(2)	0.2624(1)	0.0337
O(130)	−0.0784(3)	0.2762(2)	0.3309(2)	0.0409
O(140)	−0.2781(3)	−0.0151(2)	0.0601(1)	0.0351
O(150)	0.0341(3)	0.0215(2)	0.2320(2)	0.0405
Fe(2)	0.34224(4)	0.57880(4)	0.23729(2)	0.0264
N(1)	0.4434(2)	0.6713(2)	0.3870(1)	0.0240
C(1)	0.2400(3)	0.8178(3)	0.3608(2)	0.0335
C(2)	0.3780(3)	0.7768(2)	0.4325(2)	0.0272
C(3)	0.4385(3)	0.8380(3)	0.5330(2)	0.0339
C(4)	0.5706(3)	0.7886(3)	0.5857(2)	0.0352
C(5)	0.6386(3)	0.6811(3)	0.5379(2)	0.0327
C(6)	0.5705(3)	0.6245(2)	0.4375(2)	0.0256
C(7)	0.6289(3)	0.5068(3)	0.3740(2)	0.0304
O(11)	0.2110(2)	0.7527(2)	0.2709(1)	0.0394
O(12)	0.1680(3)	0.9155(2)	0.3937(2)	0.0446
O(71)	0.5465(2)	0.4670(2)	0.2832(1)	0.0330
O(72)	0.7481(2)	0.4570(2)	0.4138(2)	0.0430
N(11)	0.2495(2)	0.4934(2)	0.0853(1)	0.0220
C(11)	0.4373(3)	0.6819(2)	0.0627(2)	0.0248
C(12)	0.3098(3)	0.5487(2)	0.0170(2)	0.0221
C(13)	0.2560(3)	0.4889(2)	−0.0839(2)	0.0268
C(14)	0.1356(3)	0.3673(3)	−0.1145(2)	0.0301
C(15)	0.0714(3)	0.3116(2)	−0.0437(2)	0.0280
C(16)	0.1312(3)	0.3777(2)	0.0561(2)	0.0230
C(17)	0.0702(3)	0.3335(2)	0.1417(2)	0.0261
O(111)	0.4724(2)	0.7194(2)	0.1567(1)	0.0308
O(112)	0.4982(2)	0.7450(2)	0.0055(1)	0.0304
O(171)	0.1445(2)	0.4011(2)	0.2285(1)	0.0327
O(172)	−0.0508(2)	0.2348(2)	0.1187(1)	0.0316

[a] Equivalent isotropic *U*(iso) defined as one-third of the trace of the orthogonalized tensor.

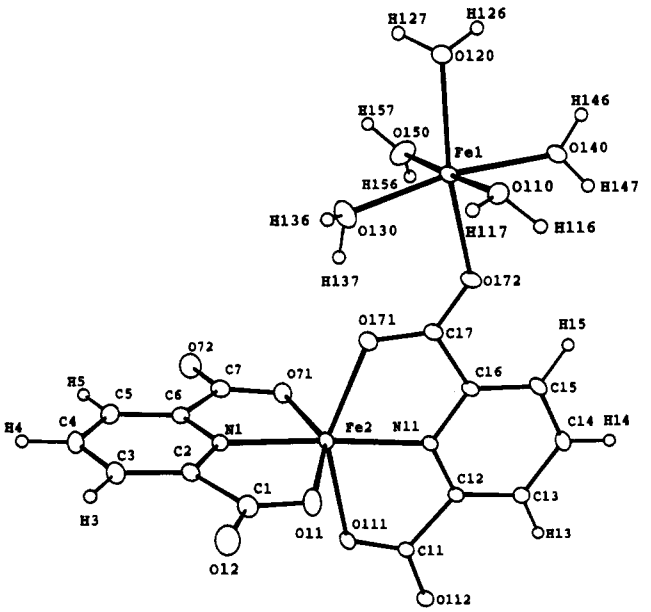

Figure 5. Structure of complex **2**.

Table 5. Selected Distances (Å) and Angles (deg) for $[(dipic)_2Fe^{II}_2(OH_2)_5]\cdot 2.25H_2O$ (**2**)

Fe(1)−O(110)	2.202(2)	Fe(2)−O(111)	2.245(2)
Fe(1)−O(120)	2.129(2)	Fe(2)−O(171)	2.204(2)
Fe(1)−O(130)	2.093(2)	C(1) −O(11)	1.258(3)
Fe(1)−O(140)	2.090(2)	C(1) −O(12)	1.251(3)
Fe(1)−O(150)	2.089(2)	C(7) −O(71)	1.276(3)
Fe(1)−O(172)	2.131(2)	C(7) −O(72)	1.235(3)
Fe(2)−N(1)	2.071(2)	C(11)−O(111)	1.258(3)
Fe(2)−O(11)	2.155(2)	C(11)−O(112)	1.245(3)
Fe(2)−O(71)	2.183(2)	C(17)−O(171)	1.258(3)
Fe(2)−N(11)	2.076(2)	C(17)−O(172)	1.248(3)
O(120)−Fe(1)−O(110)	87.07(7)	O(150)−Fe(1)−O(130)	90.00(9)
O(130)−Fe(1)−O(110)	88.09(8)	O(150)−Fe(1)−O(140)	95.52(9)
O(130)−Fe(1)−O(120)	100.47(8)	O(172)−Fe(1)−O(110)	96.60(7)
O(140)−Fe(1)−O(110)	86.91(8)	O(172)−Fe(1)−O(120)	169.21(7)
O(140)−Fe(1)−O(120)	88.23(8)	O(172)−Fe(1)−O(130)	89.81(8)
O(140)−Fe(1)−O(130)	169.73(8)	O(172)−Fe(1)−O(140)	81.87(7)
O(150)−Fe(1)−O(110)	175.98(8)	O(172)−Fe(1)−O(150)	86.93(8)
O(150)−Fe(1)−O(120)	89.80(8)		
O(11)−Fe(2)−N(1)	74.75(7)	O(111)−Fe(2)−O(71)	97.36(7)
O(71)−Fe(2)−N(1)	74.60(7)	O(111)−Fe(2)−N(11)	73.43(6)
O(71)−Fe(2)−O(11)	148.94(7)	O(171)−Fe(2)−N(1)	107.96(7)
N(11)−Fe(2)−N(1)	177.10(7)	O(171)−Fe(2)−O(11)	98.77(8)
N(11)−Fe(2)−O(11)	105.11(7)	O(171)−Fe(2)−O(71)	95.25(7)
N(11)−Fe(2)−O(71)	105.25(7)	O(171)−Fe(2)−N(11)	74.95(7)
O(111)−Fe(2)−N(1)	103.69(7)	O(171)−Fe(2)−O(111)	148.03(6)
O(111)−Fe(2)−O(11)	85.10(8)		

Table 6. Hydrogen Bonds (Å) in **2**

O(12)−H(157)	1.874(4)	O(12)−O(150)	2.744(3)
O(12)−H(202)	1.99(4)	O(12)−O(200)	2.855(3)
O(71)−H(117)	2.00(4)	O(71)−O(110)	2.747(2)
O(72)−H(136)	1.77(4)	O(72)−O(130)	2.664(3)
O(111)−H(126)	2.01(4)	O(111)−O(120)	2.771(2)
O(112)−H(116)	1.78(4)	O(112)−O(110)	2.685(2)
O(112)−H(146)	1.86(4)	O(112)−O(140)	2.680(2)
O(200)−H(127)	1.76(4)	O(200)−O(120)	2.639(3)

(2.102(2) Å), compared with Fe(2)−N(11) = 2.078(2) Å and less than 2.069(6) Å in $[(dipic)_2Fe^{II}]^{2-}$, and the loss of linearity of N−Fe−N′ with an angle N(1)−Fe(2)−N(11) = 164.37(8)°.

The Mössbauer data (Figure 4) are in agreement with these results. Simulation of the experimental spectra at 293, 221, 149, and 80 K shows two types of iron with a 1/3−2/3 distribution, with the isomer shifts δ and quadrupolar splittings ΔE_Q for each temperature respectively as follows. 1/3 type 1 with δ (ΔE_Q) (mm s^{-1}): 1.245 (3.427), 1.291 (3.529), 1.333 (3.584), 1.353 (3.652). 2/3 type 2 with δ (ΔE_Q): 1.023 (2.236), 1.069 (2.493), 1.108 (2.768), 1.151 (2.997).

The values of δ confirm that the iron atoms are in oxidation state II. Type 2 corresponds to the two [(dipic)(dipicH)Fe^{II}] subunits (iron environment N_2O_4) with values of δ close to those observed in $[(dipic)Fe^{II}(OH_2)_3]$ (iron environment NO_5) and in $[(dipic)_2Fe^{II}]^{2-}$ (N_2O_4 iron environment). Type 1 corresponds to the less electron-rich central iron atom (iron environment O_6) with larger isomer shifts.

Regarding quadrupolar splittings, for type 2 sites we notice a lower ΔE_Q than in $[(dipic)_2Fe^{II}]^{2-}$; this decrease means that the site symmetry is higher in $[(dipic)_2(dipicH)_2Fe^{II}_3(OH_2)_4]$ than in the mononuclear compound, in agreement with the structural study. In particular, the axial compression along N(1)−Fe(2)−N(11) is partly relaxed by the protonation of one of the four carboxylates of the $[(dipic)_2Fe^{II}]$ moiety, so that, despite the loss of the C_2 axis corresponding to N(1)−N(11), the coordination sphere is closer to a regular octahedron.

For sites 1, ΔE_Q is rather high, which means an important axial distorsion. Structurally, if we consider only the bond lengths to define the distortion (and not the chemical nature of the oxygens), there is indeed an elongation along O(110)−Fe(1)−O(110′) as mentioned above.

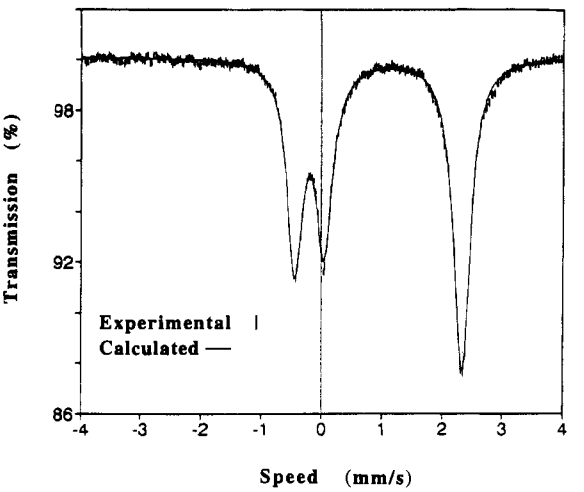

Figure 6. Mössbauer spectrum of **2** at 221 K.

Table 7. Selected Positional and Equivalent Isotropic Thermal Parameters (Å²) for $[(dipic)_4Fe^{II}_3(OH_2)_6](NH_4)_2]\cdot 4H_2O\cdot 2dipicH_2$ (**3**)

atom	*x/a*	*y/b*	*z/c*	*U*(iso)[a]
Fe(1)	0.0000	0.0000	0.0000	0.0249
O(110)	−0.0930(2)	0.1575(2)	0.0105(1)	0.0316
O(120)	0.1038(2)	0.1036(2)	0.1616(1)	0.0450
O(130)	−0.1468(2)	−0.0915(2)	0.0739(2)	0.0490
Fe(2)	−0.26551(3)	−0.57672(3)	0.22267(2)	0.0256
N(1)	−0.3018(2)	−0.5663(2)	0.0613(1)	0.0270
C(1)	−0.4916(2)	−0.7357(2)	0.0457(2)	0.0338
C(2)	−0.4120(2)	−0.6438(2)	−0.0060(2)	0.0304
C(3)	−0.4463(3)	−0.6323(3)	−0.1116(2)	0.0397
C(4)	−0.3633(3)	−0.5397(3)	−0.1447(2)	0.0447
C(5)	−0.2480(3)	−0.4608(3)	−0.0747(2)	0.0441
C(6)	−0.2203(2)	−0.4771(2)	0.0301(2)	0.0327
C(7)	−0.1043(2)	−0.3943(2)	0.1205(2)	0.0355
O(11)	−0.4435(2)	−0.7281(2)	0.1450(1)	0.0360
O(12)	−0.5968(2)	−0.8118(2)	−0.0082(1)	0.0450
O(71)	−0.1089(1)	−0.4142(1)	0.2154(1)	0.0308
O(72)	−0.0178(2)	−0.3139(2)	0.1014(2)	0.0580
N(11)	−0.2128(2)	−0.5786(2)	0.3843(1)	0.0225
C(11)	−0.1001(2)	−0.7337(2)	0.3036(2)	0.0279
C(12)	−0.1365(2)	−0.6525(2)	0.4060(2)	0.0239
C(13)	−0.0963(2)	−0.6515(2)	0.5141(2)	0.0286
C(14)	−0.1371(2)	−0.5705(2)	0.6002(2)	0.0318
C(15)	−0.2173(2)	−0.4946(2)	0.5771(2)	0.0305
C(16)	−0.2540(2)	−0.5021(2)	0.4663(2)	0.0245
C(17)	−0.3422(2)	−0.4291(2)	0.4241(2)	0.0286
O(111)	−0.1480(2)	−0.7212(2)	0.2110(1)	0.0316
O(112)	−0.0309(2)	−0.8064(2)	0.3148(1)	0.0382
O(171)	−0.3644(2)	−0.4497(2)	0.3202(1)	0.0327
O(172)	−0.3856(2)	−0.3540(2)	0.4943(1)	0.0381
N(21)	−0.2970(2)	0.0216(2)	0.4388(1)	0.0283
C(21)	−0.1878(2)	−0.1390(2)	0.3597(2)	0.0313
C(22)	−0.2175(2)	−0.0499(2)	0.4607(2)	0.0284
C(23)	−0.1671(2)	−0.0444(2)	0.5683(2)	0.0360
C(24)	−0.2010(3)	0.0386(3)	0.6568(2)	0.0431
C(25)	−0.2855(3)	0.1107(3)	0.6357(2)	0.0398
C(26)	−0.3305(2)	0.0990(2)	0.5253(2)	0.0296
C(27)	−0.4202(2)	0.1774(2)	0.4961(2)	0.0321
O(211)	−0.2296(2)	−0.1454(2)	0.2649(1)	0.0410
O(212)	−0.1116(2)	−0.2100(2)	0.3844(1)	0.0352
O(271)	−0.4486(2)	0.1791(2)	0.4011(1)	0.0415
O(272)	−0.4613(2)	0.2418(2)	0.5810(1)	0.0391

[a] Equivalent isotropic *U*(iso) defined as one-third of the trace of the orthogonalized tensor.

Magnetic susceptibility measurements show a constant effective magnetic moment between 50 and 300 K. At 300 K, $\mu_{eff} = 9.45\ \mu_B$, which is consistent with three high-spin ($S = 2$) iron(II) centers without interaction. At low temperatures, μ_{eff} first decreases until 9.12 μ_B at 9 K and finally increases again for $T < 9$ K.

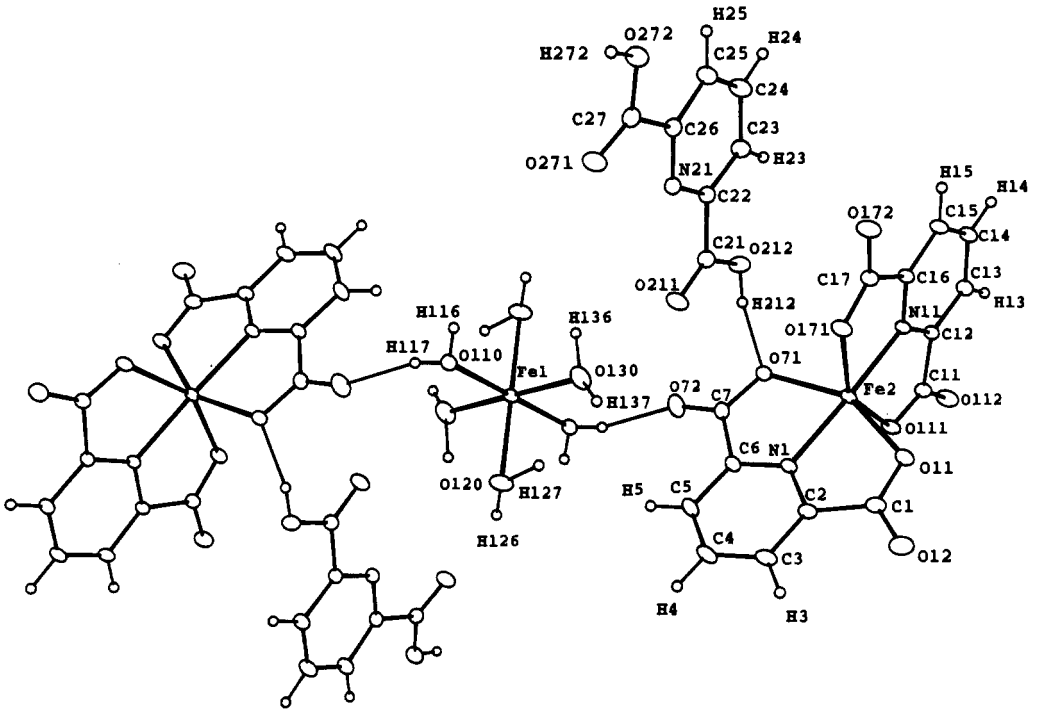

Figure 7. View of unit cell contents for **3** showing the hydrogen bonding between the molecules. The structure is symmetrical with respect to a crystallographic inversion center on Fe(1).

Table 8. Selected Distances (Å) and Angles (deg) for $[(dipic)_4Fe^{II}_3(OH_2)_6](NH_4)_2]\cdot 4H_2O\cdot 2dipicH_2$ (**3**)

Fe(1)−O(110)	2.161(2)	C(7)−O(72)	1.218(3)
Fe(1)−O(120)	2.094(2)	C(11)−O(111)	1.283(2)
Fe(1)−O(130)	2.114(2)	C(11)−O(112)	1.230(2)
C(1) −O(11)	1.279(3)	C(17)−O(171)	1.258(2)
C(1)−O(12)	1.238(3)	C(17)−O(172)	1.246(2)
C(7)−O(71)	1.281(3)		
Fe(2)−N(1)	2.075(2)	Fe(2)−O(171)	2.149(2)
Fe(2)−O(11)	2.152(2)	C(21)−O(211)	1.212(3)
Fe(2)−O(71)	2.179(2)	C(21)−O(212)	1.317(2)
Fe(2)−N(11)	2.068(2)	C(27)−O(271)	1.213(3)
Fe(2)−O(111)	2.222(1)	C(27)−O(272)	1.297(3)
O(120)−Fe(1)−O(110)	88.26(7)	O(130)−Fe(1)−O(110)′	91.36(7)
O(120)−Fe(1)−O(110)′	91.74(7)	O(130)−Fe(1)−O(120)	87.59(8)
O(130)−Fe(1)−O(110)	88.64(7)	O(130)−Fe(1)−O(120)′	92.41(8)
O(11)−Fe(2)−N(1)	75.44(7)	O(111)−Fe(2)−O(71)	95.81(6)
O(71)−Fe(2)−N(1)	74.67(6)	O(111)−Fe(2)−N(11)	74.17(6)
O(71)−Fe(2)−O(11)	150.06(6)	O(171)−Fe(2)−N(1)	106.33(6)
N(11)−Fe(2)−N(1)	175.06(7)	O(171)−Fe(2)−O(11)	92.48(7)
N(11)−Fe(2)−O(11)	109.20(6)	O(171)−Fe(2)−O(71)	94.16(6)
N(11)−Fe(2)−O(71)	100.73(6)	O(171)−Fe(2)−N(11)	75.54(6)
O(111)−Fe(2)−N(1)	104.23(6)	O(171)−Fe(2)−O(111)	149.37(6)
O(111)−Fe(2)−O(11)	93.14(6)		

The detailed interpretation of this magnetic behavior is outside the scope of this paper. Qualitatively, the peculiar law of variation of μ_{eff} at low temperature could be due to antiferromagnetic coupling inside the trinuclear species (see ref 2 for an analogous case) or alternatively to the effect of zero-field splitting or paramagnetic impurities.

$[(dipic)_2Fe^{II}_2(OH_2)_5]$ (2). Reaction of Mohr's salt and partially neutralized $dipicH_2$ acid at pH 6.25 gave the dinuclear neutral complex $\{[(dipic)_2Fe^{II}]-[Fe^{II}(OH_2)_5]\}$. The X-ray structure shows that this compound (Figure 5) is an asymmetric bimetallic complex containing one fragment $[(dipic)_2Fe^{II}]$ very similar to that observed in $[(dipic)_2Fe^{II}](NProp_4)_2$.[1] It shares one oxygen atom with a "$Fe^{II}(OH_2)_5$" fragment very close to that of $[Fe^{II}(OH_2)_6]$.[3] In this latter subunit the Fe−O distances

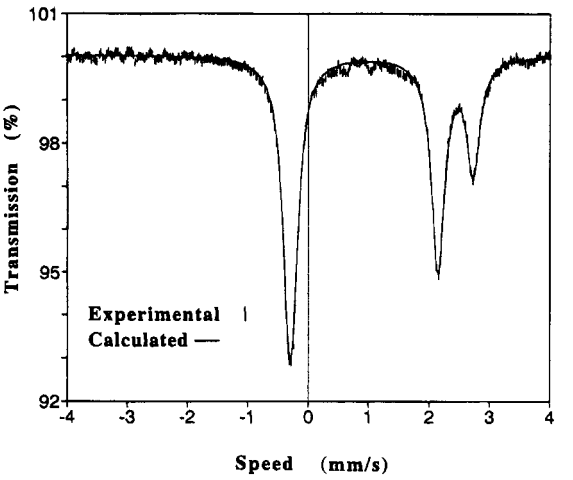

Figure 8. Experimental and calculated Mössbauer spectra of **3** at 221 K.

(Table 5) range from 2.089(2) to 2.202(2) Å with a pseudo-C_2 symmetry with respect to the Fe(1)−O(110) axis. The complexation of O(172) does not disturb the rest of the subunit $[(dipic)_2Fe^{II}]$, which has a pseudo-D_{2d} geometry with, in particular, a nearly linear N(1)−Fe(2)−N(11) arrangement [177.10(7) Å]. The molecules in the crystal are linked by a network of weak hydrogen bonds, as shown by the distances in Table 6.

This compound does not contain partially protonated dipic ligands as expected at this pH, but the nuclearity of this species shows once more that it is difficult to correlate solution chemistry and solid state structures.

The Mössbauer spectrum (Figure 6) can be fitted as two iron sites with a 50/50 distribution at different temperatures,

(2) Ménage, S.; Vitols, S. E.; Bergerat, P.; Codjovi, E.; Kahn, O.; Girerd, J.-J.; Guillot, M.; Solans, X.; Calvet, T. *Inorg. Chem.* **1991**, *30*, 2666.

(3) (a) Ruiz-Valero, C.; Monge, A.; Gutierrez-Puebla, E.; Gutierrez-Rios, E. *Acta Crystallogr.* **1984**, *40*, 811. (b) Hamalainen, R.; Turpeinen, U.; Ahlgren, M. *Eur. Cryst. Meeting* **1985**, *9*, 204. (c) Hamalainen, R.; Turpeinen, U. *Acta Chem. Scand.* **1989**, *43*, 15. (d) Strose, J.; Layten, S. W.; Strouse, C. E. *J. Am. Chem. Soc.* **1977**, *99*, 562. (e) Hamilton W. C. *Acta Crystallogr.* **1962**, *15*, 353.

Table 9. Selected Bond Distances and Angles Showing the Consequences of the Protonation of the Complexed Ligands

	Fe(3)/O(271)−C(27)−O(272)	Fe(3)/O(311)−C(31)−O(312)	Fe(5)/O(571)−C(51)−O(572)
C(1)−O(1) (Å)	1.216(9)	1.238(9)	1.238(9)
C−O(2) (Å)	1.264(9)	1.294(9)	1.277(9)
Fe−O(1) (Å)	2.214(6)	2.283(5)	2.239(6)
Fe−O(11) (Å)	2.114(5)	2.112(5)	2.157(6)
Fe−N (Å)	2.073(6)	2.088(6)	2.076(6)
N−Fe−O(1) (deg)	73.6(2)	73.0(2)	73.2(2)
N−Fe−O11 (deg)	75.9(2)	75.6(2)	75.7(2)
N−Fe−N′ (deg)	159.1(2)	159.1(2)	164.8(2)

Table 10. Selected Positional and Equivalent Isotropic Thermal Parameters (Å^2) for $[(dipic)_{10}(dipicH)_6Fe^{II}_{13}(OH_2)_{24}]\cdot 13H_2O$ (**4**)

atom	*x/a*	*y/b*	*z/c*	*U*(iso)[a]	atom	*x/a*	*y/b*	*z/c*	*U*(iso)[a]
Fe(1)	0.0000	0.0000	0.0000	0.0472	Fe(5)	−0.23356(8)	0.17999(8)	0.32414(8)	0.0400
O(110)	−0.1411(5)	0.0289(5)	0.0864(4)	0.0699	N(41)	−0.3775(4)	0.1969(4)	0.3620(4)	0.0327
O(120)	−0.0094(5)	−0.1294(4)	0.0118(4)	0.0603	C(41)	−0.3806(6)	0.3162(5)	0.4411(5)	0.0403
					C(42)	−0.4354(5)	0.2633(5)	0.4140(5)	0.0345
Fe(2)	0.25608(8)	−0.14797(8)	0.19353(8)	0.0411	C(43)	−0.5307(5)	0.2784(5)	0.4355(5)	0.0391
N(1)	0.4006(4)	−0.1660(4)	0.1496(4)	0.0331	C(44)	−0.5671(6)	0.2219(6)	0.4045(6)	0.0460
C(1)	0.3999(5)	−0.2867(5)	0.0735(5)	0.0363	C(45)	−0.5059(6)	0.1504(6)	0.3528(5)	0.0439
C(2)	0.4553(5)	−0.2356(5)	0.1009(5)	0.0329	C(46)	−0.4111(5)	0.1401(5)	0.3338(5)	0.0347
C(6)	0.4385(5)	−0.1110(5)	0.1781(5)	0.0353	C(47)	−0.3318(6)	0.0693(5)	0.2765(5)	0.0432
C(5)	0.5334(5)	−0.1265(5)	0.1589(5)	0.0397	O(411)	−0.2941(4)	0.2985(4)	0.4013(4)	0.0477
C(4)	0.5899(5)	−0.2000(6)	0.1099(5)	0.0424	O(412)	−0.4269(4)	0.3697(4)	0.5042(4)	0.0485
C(3)	0.5513(6)	−0.2555(5)	0.0796(5)	0.0433	O(471)	−0.2485(4)	0.0779(4)	0.2588(4)	0.0465
C(7)	0.3636(6)	−0.0399(5)	0.2368(5)	0.0411	O(472)	−0.3551(4)	0.0072(4)	0.2524(4)	0.0557
O(11)	0.3108(4)	−0.2596(4)	0.1076(4)	0.0458	N(51)	−0.0970(4)	0.1597(4)	0.3213(4)	0.0329
O(12)	0.4434(4)	−0.3470(4)	0.0207(4)	0.0472	C(51)	−0.0717(6)	0.2329(5)	0.1855(5)	0.0384
O(71)	0.2803(4)	−0.0418(4)	0.2510(4)	0.0486	C(52)	−0.0320(5)	0.1830(5)	0.2509(5)	0.0323
O(72)	0.3915(4)	0.0135(4)	0.2682(4)	0.0521	C(53)	0.0626(5)	0.1584(5)	0.2389(5)	0.0410
N(11)	0.1130(4)	−0.1244(4)	0.2627(4)	0.0324	C(54)	0.0878(5)	0.1125(5)	0.3035(6)	0.0388
C(11)	0.1027(7)	−0.0466(5)	0.1387(6)	0.0445	C(55)	0.0192(6)	0.0905(5)	0.3766(6)	0.0411
C(12)	0.0538(5)	−0.0775(5)	0.2268(6)	0.0345	C(56)	−0.0748(6)	0.1143(5)	0.3845(5)	0.0355
C(13)	−0.0426(6)	−0.0613(6)	0.2708(7)	0.0431	C(57)	−0.1550(6)	0.0891(5)	0.4543(5)	0.0416
C(14)	−0.0759(6)	−0.0909(6)	0.3534(8)	0.0528	O(511)	−0.1597(4)	0.2419(4)	0.2059(4)	0.0452
C(15)	−0.0152(7)	−0.1397(6)	0.3900(6)	0.0521	O(512)	−0.0172(4)	0.2616(4)	0.1197(4)	0.0496
C(16)	0.0798(6)	−0.1547(5)	0.3415(5)	0.0418	O(571)	−0.2324(4)	0.1090(4)	0.4463(4)	0.0532
C(17)	0.1555(7)	−0.2102(5)	0.3720(5)	0.0430	O(572)	−0.1395(4)	0.0437(4)	0.5166(4)	0.0461
O(111)	0.1901(5)	−0.0682(4)	0.1091(4)	0.0547					
O(112)	0.0491(5)	−0.0020(5)	0.1022(4)	0.0607	Fe(6)	−0.36367(9)	0.44012(7)	0.56590(8)	0.0416
O(171)	0.2388(5)	−0.2198(4)	0.3155(4)	0.0514	O(610)	−0.5066(4)	0.5023(4)	0.6441(4)	0.0582
O(172)	0.1301(6)	−0.2416(4)	0.4448(4)	0.0642	O(620)	−0.3705(4)	0.3536(4)	0.6696(4)	0.0498
					O(630)	−0.2229(4)	0.3740(4)	0.4925(4)	0.0490
Fe(3)	−0.31894(7)	0.68242(7)	0.80082(8)	0.0360	O(640)	−0.3103(4)	0.5204(4)	0.6204(4)	0.0535
N(21)	−0.1740(4)	0.6408(4)	0.7400(4)	0.0301	O(650)	−0.3544(5)	0.5271(4)	0.4608(4)	0.0615
C(21)	−0.1954(5)	0.5475(5)	0.8616(4)	0.0318					
C(22)	−0.1288(5)	0.5810(4)	0.7817(5)	0.0305	Fe(7)	−0.21011(8)	0.72111(8)	0.33341(8)	0.0416
C(23)	−0.0314(5)	0.5596(5)	0.7502(6)	0.0386	N(61)	−0.0744(4)	0.6708(4)	0.3285(4)	0.0363
C(24)	0.0178(5)	0.5968(5)	0.6752(6)	0.0421	C(61)	−0.0309(5)	0.7435(5)	0.1939(5)	0.0374
C(25)	−0.0294(5)	0.6582(5)	0.6323(5)	0.0391	C(62)	−0.0022(5)	0.6879(5)	0.2622(5)	0.0345
C(26)	−0.1266(5)	0.6792(5)	0.6683(5)	0.0336	C(63)	0.0899(5)	0.6571(5)	0.2588(5)	0.0400
C(27)	−0.1923(5)	0.7471(5)	0.6380(5)	0.0385	C(64)	0.1026(6)	0.6093(5)	0.3288(5)	0.0426
O(211)	−0.2822(4)	0.5820(3)	0.8817(3)	0.0377	C(65)	0.0266(6)	0.5932(6)	0.3982(6)	0.0448
O(212)	−0.1605(4)	0.4873(3)	0.9011(3)	0.0379	C(66)	−0.0620(6)	0.6246(5)	0.3961(5)	0.0390
O(271)	−0.2763(4)	0.7613(4)	0.6816(4)	0.0438	C(67)	−0.1537(6)	0.6086(6)	0.4640(5)	0.0458
O(272)	−0.1535(5)	0.7884(5)	0.5707(4)	0.0551	O(611)	−0.1181(4)	0.7646(4)	0.2111(4)	0.0456
N(31)	−0.4508(4)	0.7678(4)	0.8500(4)	0.0314	O(612)	0.0308(4)	0.7644(4)	0.1294(4)	0.0456
C(31)	−0.3733(6)	0.8522(5)	0.8980(5)	0.0417	O(671)	−0.2267(4)	0.6409(4)	0.4457(4)	0.0507
C(32)	−0.4625(6)	0.8417(5)	0.8911(5)	0.0357	O(672)	−0.1517(4)	0.5686(4)	0.5297(4)	0.0579
C(33)	−0.5504(6)	0.8956(5)	0.9266(5)	0.0436	N(71)	−0.3481(4)	0.7789(4)	0.3497(4)	0.0352
C(34)	−0.6257(6)	0.8723(6)	0.9188(5)	0.0435	C(71)	−0.3352(6)	0.6578(5)	0.2672(5)	0.0381
C(35)	−0.6128(6)	0.7963(6)	0.8750(6)	0.0447	C(72)	−0.3966(5)	0.7376(5)	0.3227(5)	0.0349
C(36)	−0.5225(5)	0.7459(5)	0.8393(5)	0.0350	C(73)	−0.4917(5)	0.7678(5)	0.3423(5)	0.0409
C(37)	−0.4943(5)	0.6616(5)	0.7883(4)	0.0315	C(74)	−0.5379(6)	0.8441(6)	0.3903(6)	0.0454
O(311)	−0.3019(4)	0.7929(3)	0.8703(4)	0.0407	C(75)	−0.4849(6)	0.8888(5)	0.4155(5)	0.0416
O(312)	−0.3782(5)	0.9217(3)	0.9373(4)	0.0489	C(76)	−0.3908(5)	0.8527(5)	0.3973(5)	0.0359
O(371)	−0.4085(4)	0.6240(3)	0.7662(4)	0.0414	C(77)	−0.3261(6)	0.8836(6)	0.4287(6)	0.0473
O(372)	−0.5531(4)	0.6367(4)	0.7696(4)	0.0470	O(711)	−0.2497(4)	0.6412(3)	0.2595(4)	0.0432
					O(712)	−0.3716(4)	0.6150(4)	0.2357(4)	0.0544
Fe(4)	−0.22352(7)	0.43224(7)	1.02311(7)	0.0332	O(771)	−0.2457(4)	0.8363(5)	0.4121(5)	0.0601
O(410)	−0.2666(4)	0.3821(4)	1.1536(3)	0.0419	O(772)	−0.3570(5)	0.9515(5)	0.4756(5)	0.0628
O(420)	−0.0850(4)	0.3980(4)	1.0260(4)	0.0449					
O(430)	−0.2078(3)	0.3110(3)	0.9724(4)	0.0417					
O(440)	−0.3640(4)	0.4686(3)	1.0169(4)	0.0446					
O(450)	−0.2485(4)	0.5554(4)	1.0758(4)	0.0517					

[a] Equivalent isotropic *U*(iso) defined as one-third of the trace of the orthogonalized tensor.

respectively 293, 221, 149, and 80 K: site 1 δ (mm s^{-1}) = 1.254, 1.289, 1.319, 1.351, ΔE_Q (mm s^{-1}) = 1.955, 2.266, 2.560, 2.738; site 2 δ (mm s^{-1}) = 1.022, 1.061, 1.106, 1.147; ΔE_Q (mm s^{-1}) = 2.569, 2.839, 3.148, 3.380.

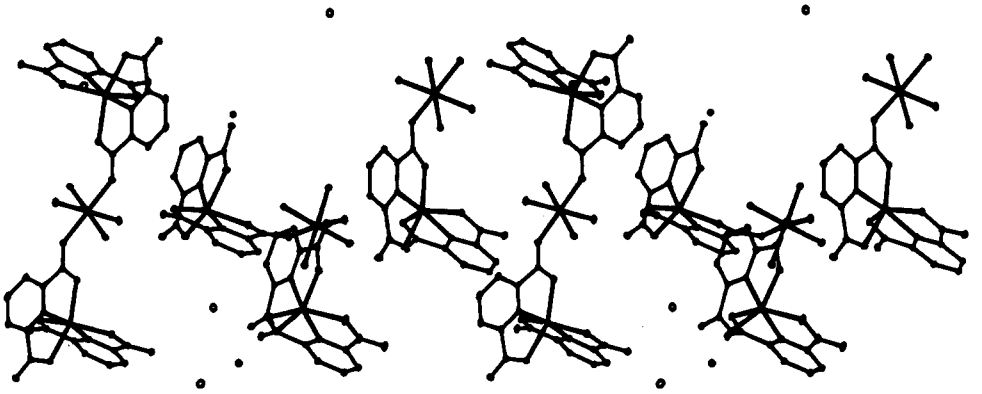

Figure 9. Stereoscopic view showing the arrangement of the various mononuclear, dinuclear, and trinuclear complexes in unit cell of **4**.

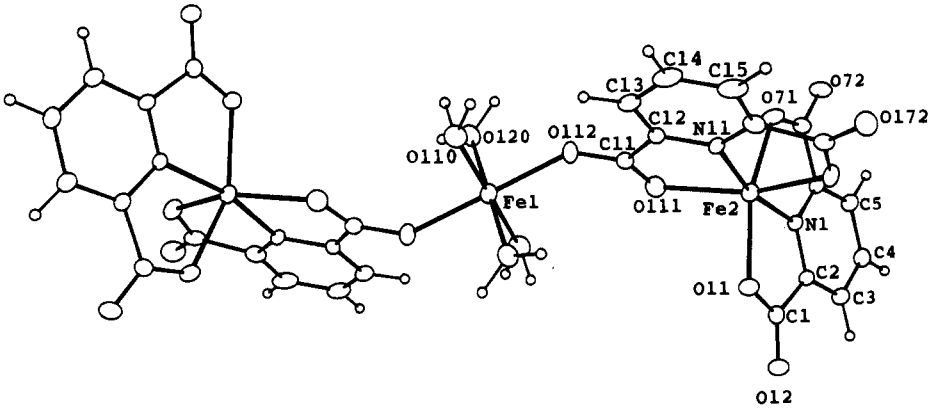

Figure 10. ORTEP drawing of the trinuclear complex of **4**: $\{[(dipic)_2Fe^{II}]-[Fe^{II}(OH_2)_4]-[Fe^{II}(dipic)_2]\}^{2-}$.

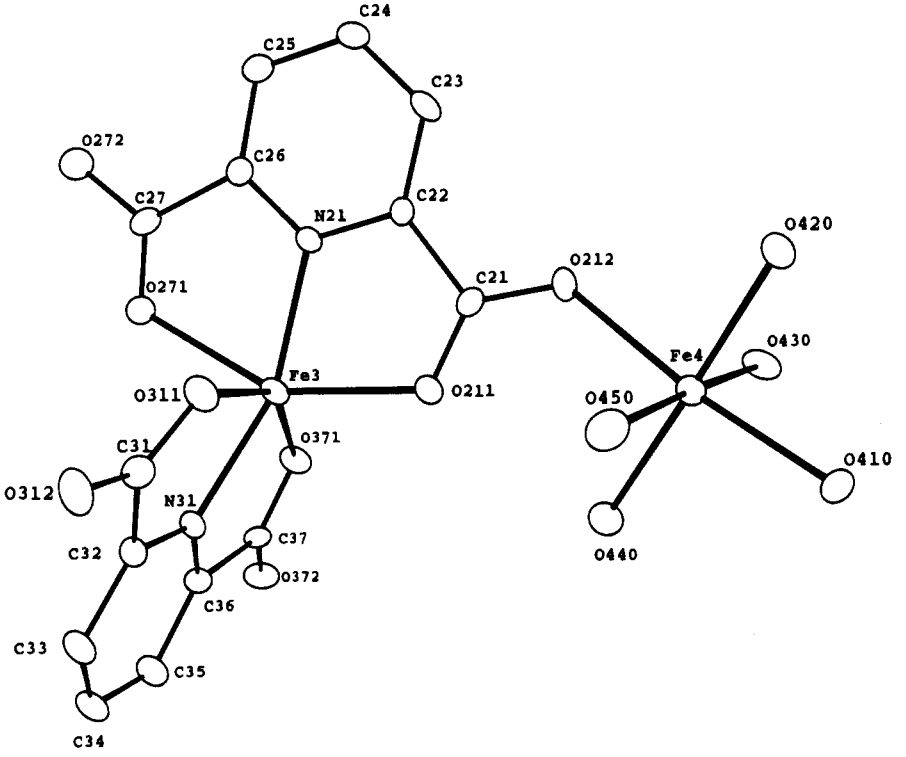

Figure 11. View the doubly protonated cationic dinuclear complex of **4**: $\{[(dipicH)Fe^{II}(dipicH)]-[Fe^{II}(OH_2)_5]\}^{2+}$. The acidic protons linked to O(272) and O(312) of the dipicH ligands have not been crystallographically located and are not shown.

The values of isomer shifts δ indicate that both iron atoms are at oxidation state II and that the iron environment of the site 1 is "FeO_6" [as in $Fe^{II}(OH_2)_5O$] while that of the site 2 is "FeN_2O_4" as in [(dipic)$_2$Fe]. For this iron atom, the values of quadrupolar splitting ΔE_Q are very close to that measured in isolated $[(dipic)_2Fe^{II}]^{2-}$, whereas for the site 1, ΔE_Q values are smaller than in $[(dipic)_2(dipicH)_2Fe^{II}_3(OH_2)_4]$, which is more distorted.

The magnetic moment of 7.722 μ_B at 300 K (5.46 μ_B per Fe(II)) shows that the iron atoms are high-spin uncoupled

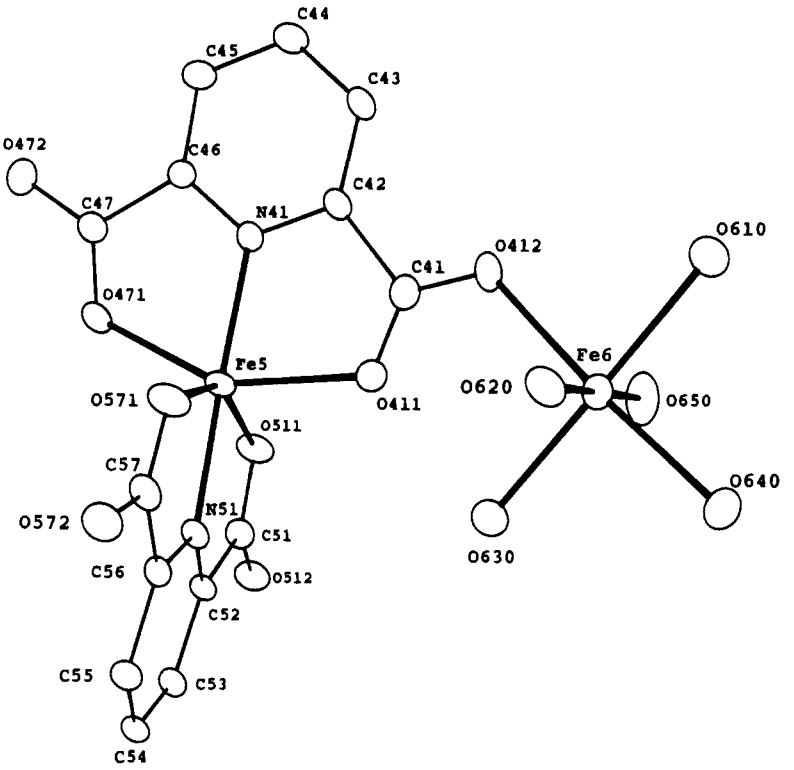

Figure 12. Structure of the singly protonated cationic dinuclear complex of **4**: $[(dipicH)Fe^{II}(dipic)]-[Fe^{II}(OH_2)_5]^+$. The acidic proton on O(572) is not shown.

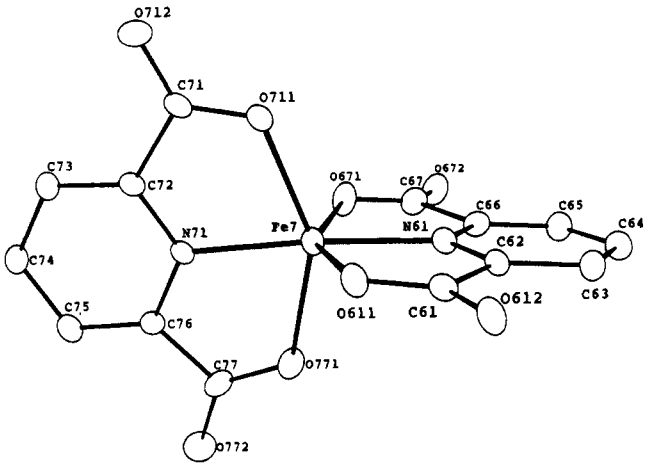

Figure 13. Molecular structure of the mononuclear anionic complex of **4**: $[(dipic)_2Fe^{II}]^{2-}$.

Fe(II). The very slow decrease down to 60 K (5.46 μ_B per Fe(II)) is probably due to temperature-independent paramagnetism whereas the drop between 60 and 5 K (4.354 μ_B per Fe(II)) can be explained by weak hydrogen bonding and/or zero-field splitting as in the previous case.

$[(dipic)_4Fe^{II}_3(OH_2)_6](NH_4)\cdot 4H_2O\cdot 2dipicH_2$ (3). Under nearly the same conditions as for the previous compound, except the pH which was 5.85 instead of 6.25, the reaction gave an orange-red crystalline solid.

Figure 7 shows a part of the unit cell, which contains one cation $[Fe^{II}(OH_2)_6]^{2+}$, two anions $[(dipic)_2Fe^{II}]^{2-}$, two $dipicH_2$, two ammonium cations, and four water molecules. *Thus, very astonishingly, the structure encompasses both reactants and products of complexation as if the solution had been frozen during the reaction! Such an observation is unique to our knowledge.*

$[Fe^{II}(OH_2)_6]^{2+}$ is a nearly perfect octahedron with Fe–O bond distances (Table 8) ranging from 2.094(2) to 2.161(2) Å and with O–Fe–O angles from 87.59(7) to 92.41(8)°, very similar to that found in other compounds.[3] This cation is linked to the anion $[(dipic)_2Fe^{II}]^{2-}$ through hydrogen bonding as indicated by the distances O–O and the angles O–H–O: O(130)–O(12) = 2.667(3) Å, H(137)–O(12) = 1.71(4) Å; O(110)–O(72) = 2.661(3) Å, H(117)–O(72) = 1.86(4) Å. This latter anion, whose geometry is very similar to that of previously observed, is also linked by hydrogen bonding to acid molecules $dipicH_2$ as shown by the O–O and O–H distances O(71)–H(212) = 1.78(4) Å, O(71)–O(212) = 2.649(2) Å, O(172)–H(272) = 1.67(4) Å, and O(172)–O(272) = 2.517(2) Å. Each $dipicH_2$ is also linked to an ammonium cation with O(271)–H(104) = 1.87(4) Å and O(272)–N(100) = 2.795(3) Å. These acid molecules are in a planar conformation with a maximum deviation from the aromatic ring plane less than 0.15 Å. Furthermore, this plane is parallel to one of the dipic planes of $[(dipic)_2Fe^{II}]^{2-}$ with an angle of 3.0° between the mean planes.

The Mössbauer spectrum (Figure 8) shows two sites with 1/3–2/3 ratios and the following values for δ and ΔE_Q (mm s^{-1}): 2/3 of "FeN_2O_4" with δ = 1.005, 1.023, 1.052, 1.098; ΔE_Q = 2.255, 2.462, 2.655, 2.923; 1/3 of "FeO_6" with δ = 1.242, 1.349, 1.410, 1.425; ΔE_Q = 2.675, 2.972, 3.171, 3.414.

The ΔE_Q values for "FeN_2O_4" are very close to those observed for similar subunits in the previous compounds. For the other site, the ΔE_Q values are intermediate between those observed in $[(dipic)_2Fe^{II}_2(OH_2)_5]$ and in $[(dipic)_2(dipicH)_2Fe^{II}_3(OH_2)_4]$; this is due to an elongation along the O(110)–Fe(1) direction, smaller than in $[(dipic)_2(dipicH)_2Fe^{II}_3(OH_2)_4]$ but larger than in $[(dipic)_2Fe^{II}_2(OH_2)_5]$.

The magnetic moment is 9.287 μ_B at 300 K (5.36 μ_B per Fe(II)). This value drops slowly down to 50 K and then more rapidly below this temperature (3.48 μ_B per Fe(II) at 2 K) probably because of the tight hydrogen-bond network.

$[(dipic)_{10}(dipicH)_6Fe^{II}_{13}(OH_2)_{24}]\cdot 13H_2O$ (4). At slightly more acidic pH (5.65), "rapid" crystallization gave a first crop

Table 11. Selected Bond Distances (Å) and Angles (deg) for $[(dipic)_{10}(dipicH)_6Fe^{II}_{13}(OH_2)_{24}]\cdot 13H_2O$ (**4**)

Fe(1)−O(110)	2.095(6)	Fe(3)−N(21)	2.073(6)	Fe(4)−O(440)	2.186(5)	Fe(6)−O(610)	2.155(6)
Fe(1)−O(120)	2.075(6)	Fe(3)−O(211)	2.114(5)	Fe(4)−O(450)	2.087(6)	Fe(6)−O(620)	2.096(6)
Fe(1)−O(112)	2.104(6)	Fe(3)−O(271)	2.214(6)			Fe(6)−O(630)	2.130(6)
		Fe(3)−N(31)	2.088(6)	Fe(5)−N(41)	2.059(6)	Fe(6)−O(640)	2.092(6)
Fe(2)−N(1)	2.058(6)	Fe(3)−O(311)	2.283(5)	Fe(5)−O(411)	2.161(6)	Fe(6)−O(650)	2.113(6)
Fe(2)−O(11)	2.154(6)	Fe(3)−O(371)	2.112(5)	Fe(5)−O(471)	2.115(6)		
Fe(2)−O(71)	2.166(6)	C(21)−O(211)	1.267(8)	Fe(5)−N(51)	2.076(6)	Fe(7)−N(61)	2.066(7)
Fe(2)−N(11)	2.055(6)	C(21)−O(212)	1.251(8)	Fe(5)−O(511)	2.157(6)	Fe(7)−O(611)	2.166(6)
Fe(2)−O(111)	2.197(6)	C(27)−O(271)	1.216(9)	Fe(5)−O(571)	2.239(6)	Fe(7)−O(671)	2.134(6)
Fe(2)−O(171)	2.193(6)	C(27)−O(272)	1.264(9)	C(41)−O(411)	1.238(9)	Fe(7)−N(71)	2.066(6)
C(1)−O(11)	1.272(8)	O(212)−Fe(4)	2.105(5)	C(41)−O(412)	1.269(9)	Fe(7)−O(711)	2.160(6)
C(1)−O(12)	1.230(9)	C(31)−O(311)	1.238(9)	C(47)−O(471)	1.266(9)	Fe(7)−O(771)	2.161(6)
C(7)−O(71)	1.246(9)	C(31)−O(312)	1.294(9)	C(47)−O(472)	1.264(9)	C(61)−O(611)	1.254(9)
C(7)−O(72)	1.261(9)	C(37)−O(371)	1.260(8)	O(412)−Fe(6)	2.176(6)	C(61)−O(612)	1.225(9)
C(11)−O(111)	1.24(1)	C(37)−O(372)	1.228(8)	C(51)−O(511)	1.267(9)	C(67)−O(671)	1.28(1)
C(11)−O(112)	1.269(9)			C(51)−O(512)	1.235(9)	C(67)−O(672)	1.223(9)
C(17)−O(171)	1.27(1)	Fe(4)−O(410)	2.151(5)	C(57)−O(571)	1.238(9)	C(71)−O(711)	1.264(9)
C(17)−O(172)	1.221(9)	Fe(4)−O(420)	2.133(5)	C(57)−O(572)	1.277(9)	C(71)−O(712)	1.232(9)
		Fe(4)−O(430)	2.077(5)			C(77)−O(771)	1.25(1)
						C(77)−O(772)	1.262(9)

O(120)−Fe(1)−O(110)	86.7(3)	N(31)−Fe(3)−N(21)	159.1(2)	O(450)−Fe(4)−O(430)	176.3(2)	O(640)−Fe(6)−O(412)	173.7(2)
O(120)−Fe(1)−O(110)′	93.3(3)	N(31)−Fe(3)−O(211)	118.8(2)	O(450)−Fe(4)−O(440)	88.1(2)	O(640)−Fe(6)−O(610)	91.2(2)
O(112)−Fe(1)−O(110)	91.9(3)	N(31)−Fe(3)−O(271)	91.0(2)			O(640)−Fe(6)−O(620)	89.9(2)
O(112)−Fe(1)−O(110)′	88.1(3)	O(311)−Fe(3)−N(21)	91.4(2)	O(411)−Fe(5)−N(41)	74.3(2)	O(640)−Fe(6)−O(630)	89.3(2)
O(112)−Fe(1)−O(120)	84.8(3)	O(311)−Fe(3)−O(211)	96.1(2)	O(471)−Fe(5)−N(41)	76.4(2)	O(650)−Fe(6)−O(412)	85.2(3)
O(112)−Fe(1)−O(120)′	95.2(3)	O(311)−Fe(3)−O(271)	85.8(2)	O(471)−Fe(5)−O(411)	150.4(2)	O(650)−Fe(6)−O(610)	94.5(3)
		O(311)−Fe(3)−N(31)	73.0(2)	N(51)−Fe(5)−N(41)	164.8(2)	O(650)−Fe(6)−O(620)	179.1(3)
O(11)−Fe(2)−N(1)	74.7(2)	O(371)−Fe(3)−N(21)	119.4(2)	N(51)−Fe(5)−O(411)	98.6(2)	O(650)−Fe(6)−O(630)	87.9(2)
O(71)−Fe(2)−N(1)	75.0(2)	O(371)−Fe(3)−O(211)	97.5(2)	N(51)−Fe(5)−O(471)	110.9(2)	O(650)−Fe(6)−O(640)	89.6(3)
O(71)−Fe(2)−O(11)	149.6(2)	O(371)−Fe(3)−O(271)	96.4(2)	O(511)−Fe(5)−N(41)	117.8(2)		
N(11)−Fe(2)−N(1)	167.6(2)	O(371)−Fe(3)−N(31)	75.6(2)	O(511)−Fe(5)−O(411)	94.9(2)	O(611)−Fe(7)−N(61)	74.3(2)
N(11)−Fe(2)−O(11)	114.5(2)	O(371)−Fe(3)−O(311)	148.6(2)	O(511)−Fe(5)−O(471)	94.6(2)	O(671)−Fe(7)−N(61)	75.3(2)
N(11)−Fe(2)−O(71)	95.8(2)			O(511)−Fe(5)−N(51)	75.7(2)	O(671)−Fe(7)−O(611)	149.1(2)
O(111)−Fe(2)−N(1)	115.0(2)	O(410)−Fe(4)−O(212)	169.0(2)	O(571)−Fe(5)−N(41)	92.7(2)	N(71)−Fe(7)−N(61)	173.9(2)
O(111)−Fe(2)−O(11)	93.5(2)	O(420)−Fe(4)−O(212)	85.6(2)	O(571)−Fe(5)−O(411)	87.8(2)	N(71)−Fe(7)−O(611)	108.4(2)
O(111)−Fe(2)−O(71)	96.8(2)	O(420)−Fe(4)−O(410)	84.8(2)	O(571)−Fe(5)−O(471)	98.1(2)	N(71)−Fe(7)−O(671)	102.5(2)
O(111)−Fe(2)−N(11)	73.8(2)	O(430)−Fe(4)−O(212)	95.0(2)	O(571)−Fe(5)−N(51)	73.3(2)	O(711)−Fe(7)−N(61)	111.3(2)
O(171)−Fe(2)−N(1)	96.6(2)	O(430)−Fe(4)−O(410)	90.7(2)	O(571)−Fe(5)−O(511)	149.0(2)	O(711)−Fe(7)−O(611)	88.5(2)
O(171)−Fe(2)−O(11)	96.9(2)	O(430)−Fe(4)−O(420)	91.7(2)			O(711)−Fe(7)−O(671)	97.9(2)
O(171)−Fe(2)−O(71)	89.1(2)	O(440)−Fe(4)−O(212)	93.0(2)	O(610)−Fe(6)−O(412)	85.7(2)	O(711)−Fe(7)−N(71)	74.5(2)
O(171)−Fe(2)−N(11)	74.7(2)	O(440)−Fe(4)−O(410)	96.6(2)	O(620)−Fe(6)−O(412)	95.3(2)	O(771)−Fe(7)−N(61)	99.8(2)
O(171)−Fe(2)−O(111)	148.4(2)	O(440)−Fe(4)−O(420)	178.6(2)	O(620)−Fe(6)−O(610)	86.3(2)	O(771)−Fe(7)−O(611)	99.2(3)
		O(440)−Fe(4)−O(430)	88.3(2)	O(630)−Fe(6)−O(412)	94.1(2)	O(771)−Fe(7)−O(671)	90.9(3)
O(211)−Fe(3)−N(21)	75.9(2)	O(450)−Fe(4)−O(212)	86.2(2)	O(630)−Fe(6)−O(610)	177.5(2)	O(771)−Fe(7)−N(71)	74.5(2)
O(271)−Fe(3)−N(21)	73.6(2)	O(450)−Fe(4)−O(410)	88.7(2)	O(630)−Fe(6)−O(620)	91.3(2)	O(771)−Fe(7)−O(711)	148.9(2)
O(271)−Fe(3)−O(211)	149.5(2)	O(450)−Fe(4)−O(420)	91.8(2)				

(yield 70%) of a dark-purplish solid first formulated as $[(dipic)_{16}Fe^{II}_{13}(OH_2)_{37}]$. The compound crystallizes in the space group $P\bar{1}$ with 6.5 interstitial water molecules per asymmetric unit. Successive difference Fourier syntheses and refinements revealed half a trinuclear complex "$(dipic)_4Fe_3(OH_2)_4$" around an inversion center, two dinuclear complexes "$(dipic)_2Fe^{II}_2(OH_2)_5$", and one dinuclear "$(dipic)_2Fe^{II}$" per asymmetric unit. Mössbauer and magnetic studies indicated that all the iron atoms were at the oxidation state 2+ (see below). Electroneutrality of the crystals therefore requires to counterbalance 6.5 times two positive charges coming from the iron(II) atoms minus 8 times the two negative charges brought by the $dipic^{2-}$, which gives an excess of 3 negative charges per asymmetric unit. These charges are compensated by three protons, either on dipic ligands or on water molecules, which could not be located without any ambiguity on the Fourier maps. It must be remembered that 1026 electrons were located at this stage and that the Fourier difference contrast was not high enough to place the three last electrons. However, as emphasized for the structure of $[(dipic)_2(dipicH)_2Fe^{II}_3(OH_2)_4]$ described above, the geometric changes induced by protonation (Figure 3) on a dipic/Fe complex are large enough to allow some discrimination. Protonation of O(2) increases **b** which becomes larger than **a**, increases **c** which becomes greater than 2.20 Å, increases Fe−N which becomes greater than 2.07 Å, and reduces N−Fe−O(1) which becomes larger then N−Fe−O(11). Additionally, N−Fe−N′ is no longer linear, with an angle value less than 170°.

According to these indications (Table 9), the three missing protons have been unambiguously assigned: two on one of the dinuclear complexes [O(272) and O(372)]; one on the other [O(572)]. The content of the electrically neutral unit cell (Figure 9) is therefore as follows: one trinuclear anionic complex $\{[(dipic)_2Fe^{II}]-[Fe^{II}(OH_2)_4]-[Fe^{II}(dipic)_2]\}^{2-}$, Figure 10; two doubly protonated cationic dinuclear complexes $\{[(dipicH)Fe^{II}(dipicH)]-[Fe^{II}(OH_2)_5]\}^{2+}$, Figure 11; two singly protonated cationic dinuclear complexes $[(dipicH)Fe^{II}(dipic)]-[Fe^{II}(OH_2)_5]^{+}$, Figure 12; two mononuclear anionic complexes $[(dipic)_2Fe^{II}]^{2-}$, Figure 13; 13 interstitial water molecules.

Selected bond distances and angles are given in Table 11. The geometry of the unprotonated trinuclear complex (Figure 10) is very close to that of $\{[(dipic)(dipicH)Fe^{II}]-[Fe^{II}(OH_2)_4]-[Fe^{II}(dipic)(dipicH)]\}$ with a central iron atom surrounded by four water molecules in the same plane, the octahedron being completed by two oxygen atoms belonging to two carboxylate groups. The geometry of this central complex is close to an octahedron with distances Fe−O from 2.075(6) to 2.104(6) Å and angles ranging from 84.8(3) to 95.2(3)°. The geometry of the trinuclear complexes is also very close to that observed in

Table 12. Angles (deg) between the dipic Mean Planes in **4** Showing That the Complexes Pack in Two Perpendicular Families

	N(11) to O(172)	N(21) to O(272)	N(31) to O(372)	N(41) to O(472)	N(51) to O(572)	N(61) to O(672)	N(71) to O(772)
N(1) to O(72)	96.9	95.3	7.0	177.9	85.4	93.8	9.5
N(11) to O(172)		167.7	95.1	83.5	168.3	8.7	99.5
N(21) to O(272)			97.1	84.2	15.6	167.3	92.5
N(31) to O(372)				171.0	88.6	91.0	5.1
N(41) to O(472)					94.5	86.3	168.4
N(51) to O(572)						176.6	84.7
N(61) to O(672)							95.2

Table 13. Hydrogen Bonds (Å) in **4**

O(612)–H(126)	1.681(5)	O(612)–O(120)	2.632(8)
O(12)–H(447)	1.683(5)	O(12)–O(440)	2.744(8)
O(171)–H(626)	1.756(5)	O(171)–O(620)	2.659(7)
O(172)–H(637)	1.649(6)	O(172)–O(630)	2.639(8)
O(372)–H(417)	1.888(5)	O(372)–O(410)	2.706(7)
O(300)–H(426)	1.822(7)	O(300)–O(420)	2.763(9)
O(612)–H(426)	1.855(5)	O(612)–O(430)	2.685(8)
O(712)–H(456)	1.911(6)	O(72)–O(450)	2.701(8)
O(472)–H(502)	1.972(6)	O(472)–O(500)	2.698(9)
O(572)–H(602)	1.360(6)	O(572)–O(600)	2.630(8)
O(200)–H(627)	1.82(2)	O(200)–O(620)	2.74(2)
O(640)–H(647)	1.676(6)	O(640)–O(672)	2.630(8)
O(671)–H(656)	1.966(6)	O(671)–O(650)	2.92(1)
O(500)–H(401)	1.885(7)	O(500)–O(400)	2.71(2)

less symmetrical species $[(dipic)Fe^{II}(dipic)]-[Fe^{II}(OH_2)_5]$ with a fragment "$Fe^{II}(OH_2)_5O$" sharing an oxygen atom belonging to a carboxylic group.

As shown by the angles between the dipic or dipicH ligand mean planes (Table 12) and illustrated in Figure 9, the complexes lie in a nearly parallel fashion. The molecules in the cell are linked by a dense network of intermolecular hydrogen bonds as shown by the distances given in Table 13.

The Mössbauer spectrum (Figure 14) can be fitted using the values found previously for the other compounds with seven different iron sites (as follow). Three FeO_6 sites: one "$Fe^{II}(OH_2)_4O_2$" in the trinuclear $\{[(dipic)_2Fe^{II}]-[Fe^{II}(OH_2)_4]-[Fe^{II}(dipic)_2]\}^{2-}$ complex similar to $[(dipic)_2(dipicH)_2Fe^{II}_3(OH_2)_4]$; one "$Fe(OH_2)_5O$" similar to that of $[(dipic)_2Fe^{II}_2(OH_2)_5]$ in each dinuclear complex. Four FeN_2O_4 sites in the protonated dinuclear and in the mononuclear complexes close to $[(dipic)_2Fe^{II}]^{2-}$: one free $[(dipic)_2Fe^{II}]^{2-}$; one "$(dipic)_2Fe^{II}$" in the trinuclear complex; one "$[(dipic)(dipicH)Fe^{II}]$" and one "$(dipicH)_2Fe^{II}$" in the dinuclear complexes.

Due to the extreme complexity of this system, the abundance of each site has been fixed from the crystal structure. Initial values of δ and ΔE_Q were introduced from the fits of structurally related compounds and then allowed to refine. Values of δ and ΔE_Q (mm s^{-1}) obtained after refinement, are given Table 14.

The magnetic moment is 19.679 μ_B (i.e. 5.438 μ_B per Fe(II)). Due to temperature independent paramagnetism, this value decreases steadily down to 55 K (5.26 μ_B per Fe(II)) and very rapidly below this value (3.36 μ_B per Fe(II) at 2 K) on account of intermolecular hydrogen bonds.

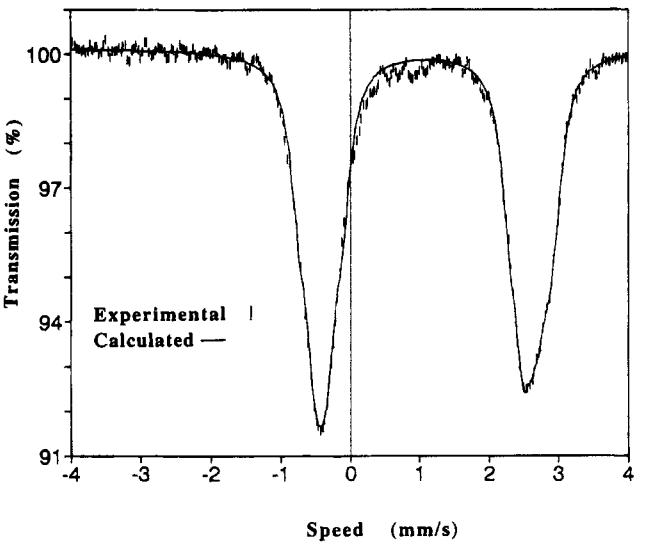

Figure 14. Mössbauer spectrum of **4** at 80 K.

Table 14. Mössbauer Isomer Shifts δ and Quadrupolar Splittings ΔE_Q in Parentheses as a Function of the Temperature for the Seven Sites in **4** (mm s^{-1})

	293 K	221 K	149 K	80 K
site A	1.295 (2.973)	1.364 (3.136)	1.311 (3.417)	1.339 (3.291)
site B	1.077 (2.369)	1.055 (2.799)	1.101 (2.792)	1.111 (2.911)
site C	1.042 (2.442)	0.978 (2.339)	1.025 (2.513)	1.074 (2.667)
site D	1.044 (2.011)	1.107 (2.399)	1.146 (2.600)	1.214 (2.799)
site E	1.097 (2.722)	1.152 (3.278)	1.170 (3.465)	1.177 (3.609)
site F	1.273 (1.740)	1.252 (2.208)	1.325 (2.559)	1.362 (2.740)
site G	0.968 (2.464)	1.141 (2.895)	1.169 (3.123)	1.193 (3.291)

Structural Considerations. After the above structural descriptions, it is tantalizing to try to correlate them and find a rational formation mechanism. Despite several attempts, we have not been able to correlate solution chemistry and solid state structures. In particular mother solutions which turned out to yield different crystalline products gave almost identical UV–vis spectra. This can be explained by the fact that (i) either the solution compositions are very similar because these complexes are formed in narrow pH intervals (i.e. we have the same species but in slightly different proportions) and/or (ii) all the species exhibit the same chromophores and thus give similar spectra even when the solution compositions are different.

This failure is assigned to the following factors: (i) the complexes are not thermodynamically perfect (i.e. they always exist in equilibrium with small amounts of free ligand or metal, or intermediate complexes); (ii) the equilibria are labile, so that there is ample time for equibrium displacement during the crystallization process; (iii) the solid state structures show in several cases the importance of hydrogen bonds which could be the driving force for the crystallization of a given species, even if it is only a minor constituent of the mother solution.

We can however remark upon some structural "filiations", which appear compatible with the known solution chemistry.

In the species $\{[(dipic)_2Fe^{II}]-[Fe^{II}(OH_2)_5]\}$ and $\{[(dipic)(dipicH)Fe^{II}]-[Fe^{II}(OH_2)_4]-[Fe^{II}(dipic)(dipicH)]\}$ the different metal centers are linked by a *coordination bond*, so that they might exist in solution. The other two structures are more surprising because they associate in an apparently random way several building blocks (which could exist independently in

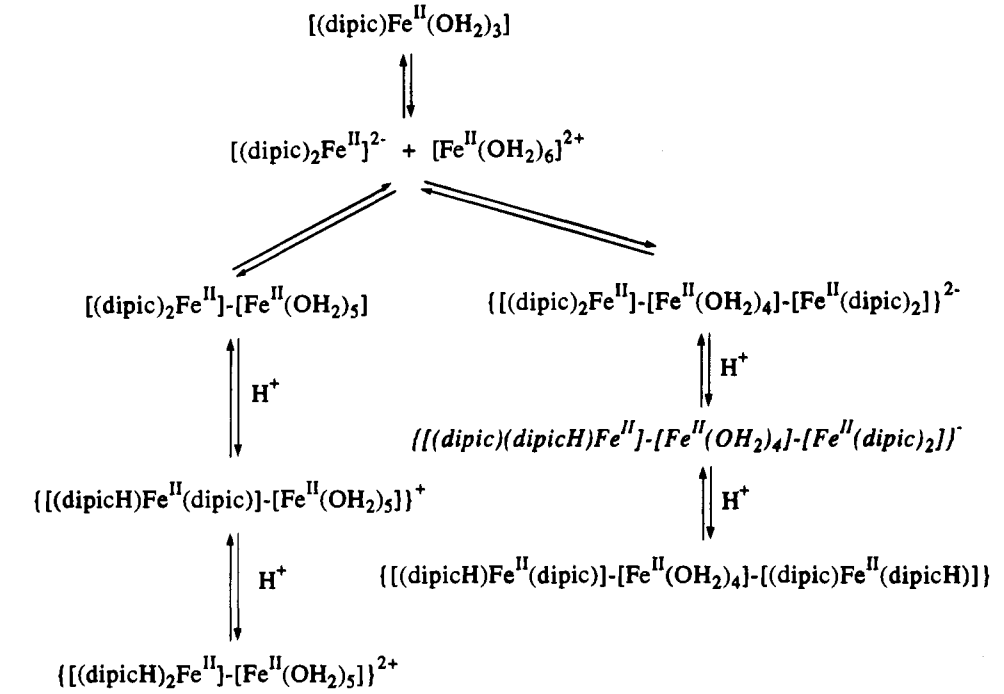

Figure 15. Relations between the various species isolated in the solid state.

solution) *through hydrogen bonds*. In $[(dipic)_4(dipicH_2)_2Fe^{II}_3(OH_2)_6](NH_4)_2{\cdot}4H_2O$ we have already mentioned this extraordinary cocrystallization of reactants and products, namely $[Fe^{II}(OH_2)_6]^{2+}$, dipicH$_2$, and $[(dipic)_2Fe^{II}]^{2-}$. In $[(dipic)_{10}(dipicH)_6Fe^{II}_{13}(OH_2)_{24}]{\cdot}13H_2O$ we find some already known building blocks (in various stages of protonation) such as $\{[(dipic)(dipicH)Fe^{II}]-[Fe^{II}(OH_2)_5]\}^+$, $\{[(dipicH)_2Fe^{II}]-[Fe^{II}(OH_2)_5]\}^{2+}$, $\{[(dipic)_2Fe^{II}]-[Fe^{II}(OH_2)_4]-[(dipic)_2Fe^{II}]\}^{2-}$, and the mononuclear $[(dipic)_2Fe^{II}]^{2-}$ species, all of them being connected by hydrogen bonds. Contrary to the first structures, the last two *overall structures* should not exist in solution, because their stabilities rely on bonds which are not stronger than the ones involved in the solvent itself.

The two compounds $\{[(dipic)_2Fe^{II}]-[Fe^{II}(OH_2)_5]\}$ and $\{[(dipic)_2Fe^{II}]-[Fe^{II}(OH_2)_4]-[Fe^{II}(dipic)_2]\}^{2-}$ can be considered as resulting from the association of a $[(dipic)_2Fe^{II}]^{2-}$ moiety *playing the role of ligand through its free oxygen carboxylate*, with an "uncomplexed" iron(II), i.e. $[Fe^{II}(OH_2)_4]^{2+}$ or $[Fe^{II}(OH_2)_5]^{2+}$. This implies formally the reaction between fragments such as $[(dipic)_2Fe^{II}]^{2-}$ and $[Fe^{II}(OH_2)_6]^{2+}$, the coexistence of which in small concentrations being possible from the equilibrium constants established by Anderegg:[4]

$$2[(dipic)Fe^{II}(OH_2)_3] \rightleftarrows [Fe^{II}(OH_2)_6]^{2+} + [(dipic)_2Fe^{II}]^{2-} \quad (2)$$

In fact, the reaction we postulate here is merely the reaction of the Lewis base $[(dipic)_2Fe^{II}]^{2-}$ (see paper 1 of this series) with Lewis acids such as $[Fe^{II}(OH_2)_5]^{2+}$ or $[Fe^{II}(OH_2)_4]^{2+}$, so that it can be legitimately assumed they can react together in solution to give the dinuclear and trinuclear species we characterized in the solid state:

$$[Fe^{II}(OH_2)_6]^{2+} + [(dipic)_2Fe^{II}]^{2-} \rightleftarrows \{[(dipic)_2Fe^{II}]-[Fe^{II}(OH_2)_5]\} + H_2O \quad (3)$$

$$\{[(dipic)_2Fe^{II}]-[Fe^{II}(OH_2)_5]\} + [(dipic)_2Fe^{II}]^{2-} \rightleftarrows \{[(dipic)_2Fe^{II}]-[Fe^{II}(OH_2)_4]-[Fe^{II}(dipic)_2]\}^{2-} + H_2O \quad (4)$$

These oligonuclear species could exist in neutral aqueous solutions and thus could be protonated in acidic medium to afford all the protonated buiding blocks that were identified, except the missing monoprotonated trinuclear complex $\{[(dipic)(dipicH)Fe^{II}]-[Fe^{II}(OH_2)_4]-[Fe^{II}(dipic)_2]\}^-$ which we did not isolate but whose existence can be reasonably assumed.

Figure 15 sums up the relations between the various species observed in the solid state. The complexity of this diagram and the large number[5] of species which can coexist in solution emphasize the fact that many precautions must be taken in dealing with iron(II)–dipic complexes for iron titration, as electron carriers, or as intermediates in catalysis. In particular, the stability of $[(dipicH)_2Fe^{II}]$ as the only catalytic intermediate in several dioxygen activation processes can be questioned.

Acknowledgment. The authors thank J.-P. Tuchagues, G. Lemercier, and A. Mari (LCC-CNRS, Toulouse, France) for helpful discussions and for measurements and simulations of the Mössbauer and magnetic data.

Supporting Information Available: Complete tables of X-ray crystallographic parameters, atom coordinates, thermal parameters, bond lengths, and bond angles for the complexes (34 pages). Ordering information is given on any current masthead page.

IC9501024

(4) Anderegg, G. *Helv. Chim. Acta* **1960**, *43*, 414.

(5) Besides, this diagram does not include the two complexes described in the following paper of this issue (*Inorg. Chem.* **1995**, *34*, 5150).